ASTRONOMY & ASTROPHYSICS
SUPPLEMENT SERIES

Astron. Astrophys. Suppl. Ser. **132**, 305–331 (1998)

Fifteen years monitoring of extragalactic radio sources at 22, 37 and 87 GHz

H. Teräsranta[1], M. Tornikoski[1], A. Mujunen[1], K. Karlamaa[1], T. Valtonen[1], N. Henelius[1], S. Urpo[1], M. Lainela[2], T. Pursimo[2], K. Nilsson[2], S. Wiren[2], A. Lähteenmäki[2], M. Korpi[2], R. Rekola[2], P. Heinämäki[2], M. Hanski[2], P. Nurmi[2], K. Kokkonen[2], P. Keinänen[2], O. Joutsamo[2], J. Oksanen[2], H. Pietilä[2], E. Valtaoja[2], M. Valtonen[2], and P. Könönen[3]

[1] Metsähovi Radio Research Station, Helsinki University of Technology, FIN-02540 Kylmälä, Finland
[2] Tuorla Observatory, FIN-21500 Piikkiö, Finland
[3] Observatory, PO Box 14, University of Helsinki, FIN-00014 Helsinki, Finland

Received February 20; accepted April 7, 1998

Abstract. Over 13600 continuum observations of extragalactic sources are presented[1]. These observations of 157 sources at 22, 37 and 87 GHz more than doubles the millimeter observations of these sources. The data are between 1990.5 and 1995.5, and combined with our earlier published data they form a 15 year database.

Key words: galaxies: active — BL Lacertae objects: general — quasars: general — radio continuum: galaxies — radio continuum: general

1. Introduction

Observing extragalactic radio sources, generally speaking quasars has, been increasingly popular during the last years due to the numerous space borne instruments dedicating a large share of their observing time to this field. Instruments like EGRET onboard the Compton GRO (gamma rays), IUE (ultraviolet), GINGA, ASCA, XTE and ROSAT (X-rays), ISO (infrared) and many others have prompted coordinated ground-based observations. Two observing windows can be covered from the ground: the radio window (below 300 GHz) and the optical window. Monitoring of extragalactic radio sources has been continued with the Metsähovi radio telescope since 1980, most of the observations being at 22 and 37 GHz. Our sample mostly consists of Northern flat spectrum sources which have at least once reached 2 Jy at 22 GHz (Valtaoja et al. 1992). At lower frequencies (5, 8 and 14 GHz) the Michigan group has been monitoring a larger sample, which also includes most of our sources, since 1965 (Aller et al. 1985). At still higher radio frequencies there are three monitoring efforts: our 90, 135 and 230 GHz monitoring of southern sources with the SEST-telescope (Tornikoski et al. 1996), the Ian Robson team working with the JCMT-telescope at 150, 230, 270 and 375 GHz (Stevens et al. 1994), as well as the IRAM-team at 90, 142 and 230 GHz (Reuter et al. 1997) and in references therein. At optical wavelengths there are several monitoring efforts concentrating on AGN, like the ones at Tuorla Observatory (Sillanpää et al. 1991), at Rosemary Hill Observatory (Webb et al. 1988), at Foggy Bottom Observatory, at Calar Alto Observatory by the Hamburg Quasar Monitoring Program (Schramm et al. 1994) and the Heidelberg group, at Asiago Observatory (Barbieri et al. 1977), at Perugia University Observatory (Fiorucci & Tosti 1996), at Torino Observatory (Villata et al. 1997), at Dodaira Station (Kikuchi 1988) and at the Yunnan Observatory (Xie et al. 1994). The Western Kentucky University has a new automated AGN monitoring program with two optical telescopes (Hackney et al. 1996). Typically the variations in AGN are slower at radio frequencies than at higher frequency bands and thus the sampling density does not have to be so high. A monthly sampling will usually be adequate for cm-observations. Below 3 mm you should have weekly observations to get most of the variations covered. At optical frequencies even faster sampling would be desired.

Send offprint requests to: H. Teräsranta
Correspondence to: hte@alpha.hut.fi

[1] The data (Table 3) are only available in electronic form at the CDS via anonymous ftp to cdsarc.u-strasbg.fr (130.79.128.5) or via http://cdsweb.u-strasbg.fr/Abstract.html

Table 1. Receiver parameters

Frequency GHz	$HPBW$	Beam separation	B(IF) MHz	$T_{\rm sys}$ K DSB
22.2	$4.0'$	$12.0'$	1000	850[a]
22.2	$4.0'$	$10.1'$	500	300[b]
36.8	$2.4'$	$6.0'$	1000	500
87.3	$1.1'$	$3.2'$	500	200

[a] Before June 1993.
[b] After June 1993.

Table 2. Parameters K_4 and K_5 with the old and new antenna

Frequency	K_4(old)	K_4(new)	K_5(old)	K_5(new)
22 GHz	4.0	3.0	0.15	0.22
37 GHz	9.1	6.5	0.15	0.22
87 GHz	46.0	17.0	0.15	0.22

2. Observations

The observations presented here were done with the Metsähovi Radio Telescope during 1990.5-1995.5 at 22, 37 and 87 GHz. The Metsähovi 13.7 m diameter ESSCO design antenna is placed inside a radome. In August 1991 the original radome was replaced with a new one. Also the reflector panels and the back structure of the antenna were replaced with more accurate ones during the summer of 1994. The receiving system parameters are listed in Table 1. The flux density scale is calibrated against DR 21, our primary calibration source. Its fluxes at 22, 37 and 87 GHz are 19.0, 17.9 and 17.0 Jy, respectively, according to Baars et al. (1977) and Ulich (1981). As secondary calibration sources we have used 3C 274 and planets like Jupiter. The receivers at 22 and 37 GHz are of a dual beam type with a ferrite swich operating at 25 Hz. At 87 GHz the beam switching at a rate of 20 Hz is performed with a rotating chopper-wheel. The old 22 GHz mixer front end receiver was replaced with a more sensitive one with a low noise HEMT amplifier as a first stage in June 1993. The 37 GHz receiver is a mixer front end receiver operating at room temperature. The 87 GHz receiver is a Schottky mixer front end receiver cooled to 20 K.

3. Data reduction

The data reduction is similar to the one described in Teräsranta et al. (1992), although the upgrading of the antenna lead to changes in some parameters. The flux-calculating procedure is done with Eqs. (1) to (5). The error estimate for the flux is from Eq. (6), where the relative errors of the optical depth, noise tube calibration and flux integreation have been quadratically added.

$$S = K_1 K_2 K_3 \frac{U}{U_{\rm cal}} {\rm e}^{\frac{\tau}{\sin(el)}} \quad (1)$$

$$K_2 = \frac{1}{(1 - K_4(P - P_{\rm opt})^2)} \quad (2)$$

$$P_{\rm opt} = P_0 - K_5 \sin(el) - K_6 T \quad (3)$$

$$K_3 = 1 + (\theta/HPBW)^2, \text{ for Gaussian sources} \quad (4)$$

$$K_3 = (\theta/0.6/HPBW)^2/(1 - {\rm e}^{-(\theta/0.6/HPBW)^2)}, \quad (5)$$

for planets

$$\delta S = S\sqrt{(\delta U/U)^2 + (\delta\tau/\sin(el))^2 + (\delta Cal/Ucal)^2}). \quad (6)$$

In the formulae,

S	the flux density in Jy
U	the observed voltage from the A/D converter
$U_{\rm cal}$	the exess voltage coming from the noise tube calibration
K_1	the factor for converting receiver voltages to Janskys
τ	the optical depth of the atmosphere
el	the elevation angle during the observation
K_2	the correction for the antenna focusing
K_3	the correction factor for source size
K_4	the frequency dependent focus sharpness factor
K_5	the elevation dependent factor of the focus
K_6	the temperature dependent factor of the focus
P	the position of the subreflector during the observation(milli-inch)
$P_{\rm opt}$	the optimal position of the subreflector during the observation(milli-inch)
P_0	the position of the receiver focus in respect to the antenna focus (milli-inch)
T	the physical temperature of the antenna (0°C)
θ	the source diameter
$HPBW$	the antenna half power beam width
δS	the error estimate for the observation
δU	the rms error of the integration
$\delta\tau$	the error of the estimation of the optical depth
δCal	the error of the noise tube calibration.

The optimal position of the antenna focus is a function of the elevation angle and temperature according to Eq. (3). Two fixed positions for the focus were used, one for the summer and one for the winter. This kept the correction factor K_2 still quite small at the used elevation range from 20 to 70 degrees. As the corrections for the focus-offset are larger at higher frequencies, the results at 87 GHz are more severely affected. In Table 2. the values of the parameters K_4 and K_5 are tabulated at each observing frequency with the old (before summer 1994) and new antenna (after summer 1994). The parameter K_6 was the same 0.0025 with both antennas.

4. Results

The list of sources with classification and number of observations at each frequency is shown in Table 3. In the

source classification HPQ states that the source has been recorded at least once an optical polarization level equal or above 3.0%, for the LPQ type sources the polarization level has allways been below 3.0%. BL Lac type object are identified with BLO and galaxies with GAL. Sources with no classification have no optical polarization observation from the literature or have simply no optical counterpart like NRAO 150. Due to the large number of data points (over 13000), the numerical tables are available only in electronic form at the CDS via anonymous ftp. The data in Table 4 consists of date (year, month, day and hour(ut)) and the flux (Jy) and 1 sigma error estimate (Jy). There are 157 sources in Table 4, from which about 85 belong to our main sample. Some additional sources have also been observed during many multifrequency campaigns, but that data will be published elsewhere. The flux curves for the 44 best observed sources are given in Fig. 1. The numerical values for some sources during 1988 and 1989 in Fig. 1 are found in Wiren et al. (1992). The flux curves in the figures contain the whole 15 year span of our observations. The numerical values for the observations prior 1990.5 can be found in Salonen et al. (1987), Teräsranta et al. (1987) and Teräsranta et al. (1992). The flux densities in Fig. 1 are weekly mean values to allow an easier examination of the flux development. For many sources there are long periods of daily observations, which can be found in Table 4.

Generally the sources seem to vary on these frequencies on a monthly basis, the shorter variations are usually within the error bars. In some cases, like in 0202+149, there was one considerably higher flux point. When combined with another observation within a week for the figure it produced a giant error bar. Another example is in OL 093 where we also had an anomalous high value. These have been carefully checked and as no fault was found they remain in the database. At our highest observing frequency (87 GHz), the poor antenna surface accuracy prior to summer 1994 limited the observations to only a few sessions.

Acknowledgements. This work has been supported by the Academy of Finland.

References

Aller H.D., Aller M.F., Latimer G.E., Hodge P.E., 1985, ApJS 59, 513
Baars J.W.M., Gentzel R., Pauline-Toth I.I.K., Witzel A., 1977, A&A 61, 99
Barbieri C., Romano G., Di Serego A., et al., 1977, A&A 59, 419
Fiorucci M., Tosti G., 1996, A&AS 117, 475
Hackney R., Hackney K., Scott R., et al., 1996, at Blazar Continuum Variability conference, PASPC 110, p. 166
Kikuchi S., 1988, Tokyo Astron. Bull., No. 281, p. 3267
Reuter H.-P., Kramer C., Sievers A., et al., 1997, A&AS 122, 271
Salonen E., Teräsranta H., Urpo S., et al., 1987, A&AS 70, 409
Schramm K.J., Borgeest U., Kühl D., et al., 1994, A&AS 106, 349
Sillanpää A., Mikkola S., Valtaoja L., 1991, A&AS 88, 225
Stevens J.A., Litchfield S.J., Robson E.I., et al., 1994, ApJ 437, 91
Teräsranta H., Valtaoja E., Haarala S., et al., 1987, A&AS 71, 125
Teräsranta H., Tornikoski M., Valtaoja E., et al., 1992, A&AS 94, 121
Tornikoski M., Valtaoja E., Teräsranta H., et al., 1996, A&AS 116, 157
Ulich B., 1981, AJ 86, 1619
Valtaoja E., Lähteenmäki A., Teräsranta H., 1992, A&AS 95, 73
Villata M., Raiteri C.M., Chisellinei G., et al., 1997, A&AS 121, 119
Wiren S., Valtaoja E., Teräsranta H., Kotilainen J., 1992, AJ 104, 1009
Webb J.R., Smith A.G., Leacock R.J., et al., 1988, AJ 95, 374
Xie G.Z., Li K.H., Zhang Y.H., et al., 1994, A&AS 106, 361

Table 3. Source list with classification and number of observations at each frequency

Designation	other name	classification	n22	n37	n87
0003−066		BLO	15	16	0
0007+106	III ZW 2	LPQ	62	83	0
0016+731		LPQ	40	45	0
0048−097		BLO	16	18	0
0106+013	OC 012	HPQ	49	61	0
0109+224		BLO	58	69	2
0122−003		LPQ	3	2	0
0135+476	DA 55	HPQ	66	71	4
0149+218			47	50	0
0153+744		LPQ	9	3	0
0202+149		HPQ	69	79	2
0212+735		BLO	24	17	0
0215+015		BLO	1	2	0
0218+357			20	11	0
0219+428	3C 66A	BLO	21	15	3
0221+067			1	4	0
0224+671			37	43	0
0229+131		LPQ	3	7	0
0229+341		HPQ	2	1	0
0234+285		HPQ	52	53	1
0235+164		BLO	91	105	8
0238−084		GAL	11	15	0
0248+430		LPQ	39	50	0
0300+470		BLO	8	7	0
0306+102		BLO	8	8	0
0316+413	3C 84	GAL	190	223	12
0323+022		BLO	6	2	0
0333+321	NRAO 140	LPQ	61	62	1
0336−019	CTA 26	BLO	23	26	0
0355+508	NRAO 150		62	79	1
0415+379	3C 111		15	15	0
0420−014	OA 129	HPQ	100	108	5
0422+004		BLO	45	50	0
0430+052	3C 120	GAL	88	86	1
0440−003	NRAO 190	HPQ	9	5	2
0446+112		GAL	18	11	2
0454+844		BLO	4	0	0
0454+039		LPQ	29	33	0
0458−020		HPQ	44	47	1
0528+134		LPQ	116	122	12
0552+398	DA 193	LPQ	72	80	5
0605−085		HPQ	12	15	0
0642+449	OH 471	LPQ	61	66	3
0707+476		LPQ	3	0	0
0716+714		BLO	47	49	0
0723−008			7	5	0
0723+679		LPQ	6	2	0
0735+178		BLO	74	89	6
0736+017		HPQ	54	61	5
0738+313		LPQ	4	1	0
0741−063			0	1	0
0742+103			11	6	0
0743−006		BLO	7	4	0
0748+126		LPQ	2	0	0
0754+100	OI 090.4	BLO	55	59	1
0804+499		HPQ	93	103	5
0814+425		BLO	57	68	3
0820+225		BLO	9	10	0
0823+033		HPQ	3	6	0
0827+243		LPQ	13	7	1
0828+493		BLO	9	6	0
0829+046		BLO	1	1	0
0836+710		LPQ	33	25	0
0846+513		BLO	41	40	0
0850+581		LPQ	4	2	0
0851+202	OJ 287	BLO	205	214	15
0859+470		LPQ	6	7	0
0906+430	3C 216	HPQ	12	5	0
0912+297		HPQ	2	1	0
0923+392	4C 39.25	LPQ	156	172	10
0927+352			5	3	1
0945+408		LPQ	7	6	0
0953+254		LPQ	51	55	1
0954+556		HPQ	26	23	2
0954+658		BLO	41	48	0
0957+227		BLO	5	4	0
1038+528		HPQ	5	3	0
1039+811			4	2	0
1040+123		LPQ	8	6	0
1049+215		LPQ	8	5	0
1055+018	OL 093	HPQ	53	81	0
1057+100		BLO	3	4	0
1101+384	Mark 421	BLO	49	46	6
1133+704		BLO	3	0	0
1137+660		LPQ	1	0	0
1146−037		LPQ	22	29	0
1147+245		BLO	11	9	0
1150+497		HPQ	6	2	0
1156+295	4C 29.45	HPQ	85	109	7
1215+303		BLO	8	5	0
1218+304		BLO	2	2	0
1219+285	ON 231	BLO	75	77	1
1222+216			30	23	1
1226+023	3C 273	LPQ	244	265	12
1229−021		LPQ	2	0	0
1253−055	3C 279	HPQ	199	220	11
1302−102		LPQ	3	3	0
1308+326		BLO	87	84	7
1308+328			12	7	2
1406−076			14	12	3
1413+135		BLO	88	88	4
1418+546	OQ 530	BLO	65	69	2
1502+106	OR 103	HPQ	51	53	3
1510−089		HPQ	58	100	5
1522+155		HPQ	3	2	0
1538+149	4C 14.60	BLO	66	67	1
1546+027		HPQ	0	1	0
1548+056		HPQ	5	4	0
1553+113		BLO	4	3	0
1606+106		LPQ	16	18	1
1611+343		LPQ	84	111	4
1633+382	4C 38.41	LPQ	107	142	4
1637+574	OS 562	LPQ	66	82	0

Table 3. continued

Designation	other name	classification	n22	n37	n87
1641+399	3C 345	HPQ	200	270	7
1642+690		HPQ	7	4	0
1652+398	Mark 501	BLO	57	65	1
1656+053		HPQ	0	2	0
1725+044			37	38	0
1730−130	NRAO 530		6	2	0
1739+522		HPQ	60	68	0
1741−038		HPQ	60	84	4
1749+096	OT 081	BLO	129	152	6
1749+701		BLO	13	12	0
1803+784		BLO	53	61	0
1807+698	3C 371	BLO	53	71	0
1823+568		BLO	9	5	0
1828+487	3C 380	LPQ	20	16	0
1845+797	3C 390.3	GAL	44	49	0
1901+319			12	8	1
1928+738		LPQ	65	59	0
1951+498			5	3	0
1954+513		LPQ	7	5	0
2005+403			83	108	1
2007+776		BLO	46	58	0
2021+614	OW 637	LPQ	59	55	0
2022+171			7	2	2
2030+407	CYG X-3		20	85	0
2037+511			12	7	0
2121+053		HPQ	8	7	0
2131−021		BLO	16	16	0
2134+004	OX 057	LPQ	58	82	0
2136+141	OX 161	LPQ	12	10	0
2141+175	OX 169	LPQ	11	14	0
2144+092	OX 074		9	10	0
2145+067		LPQ	125	155	2
2200+420	BL Lac	BLO	175	240	11
2201+315		LPQ	71	103	3
2216−038		LPQ	18	19	0
2223−052	3C 446	HPQ	62	82	0
2225−055		HPQ	3	1	0
2227−088		HPQ	14	18	0
2230+114	CTA 102	HPQ	89	99	4
2234+282		HPQ	11	7	0
2251+158	3C 454.3	HPQ	196	241	10
2254+074		BLO	29	38	0
2319+272			4	2	0
2344+092		LPQ	10	9	0

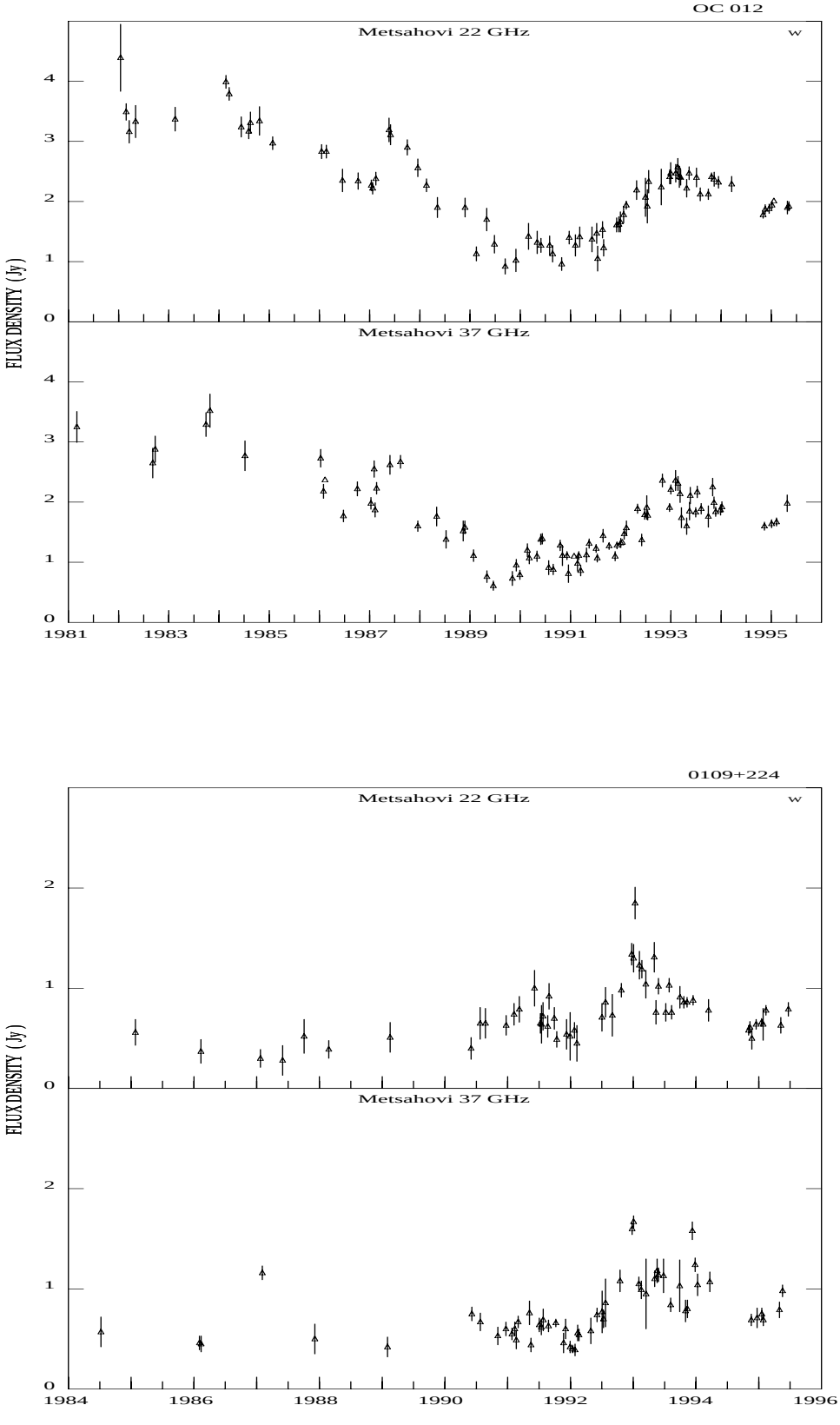

Fig. 1. Weekly mean flux density of observed sources at 22 and 37 GHz

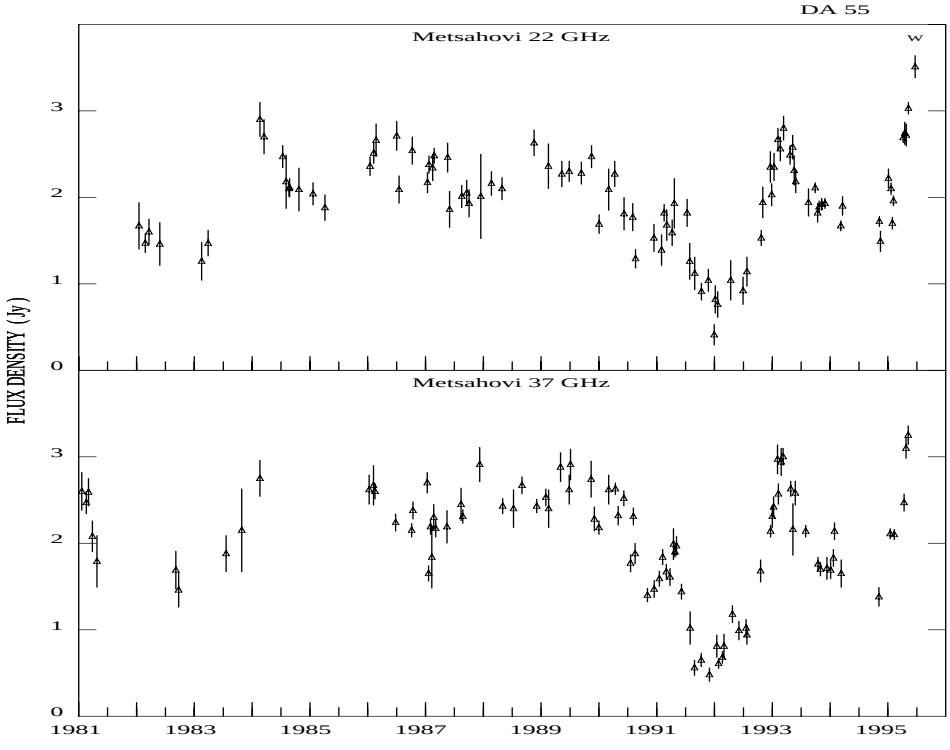

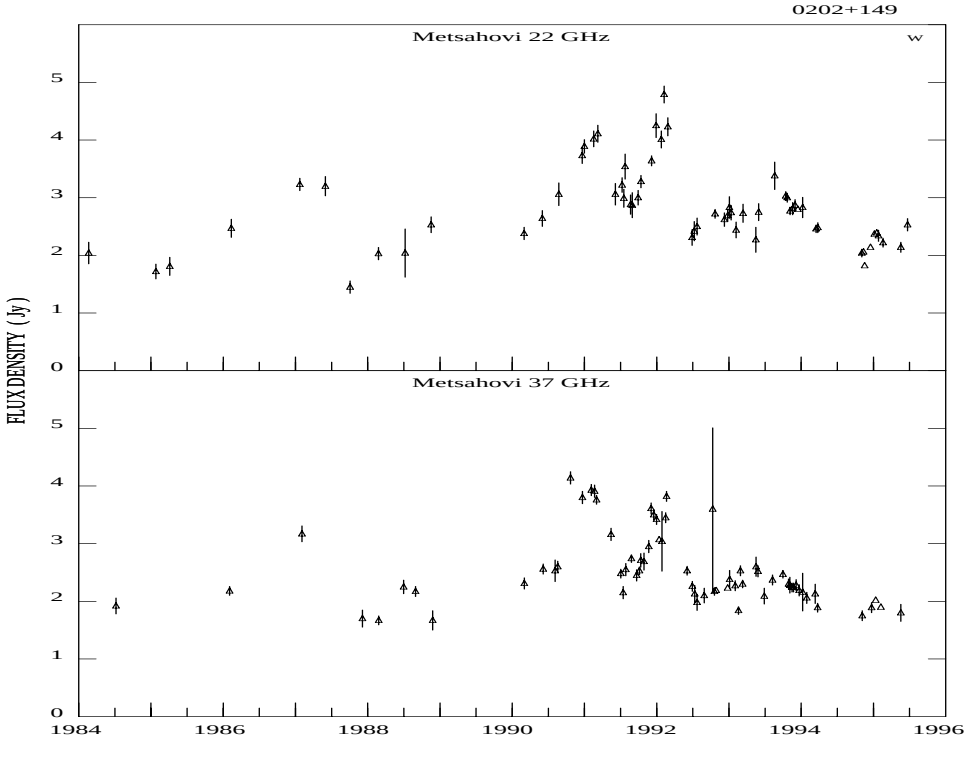

Fig. 1. continued

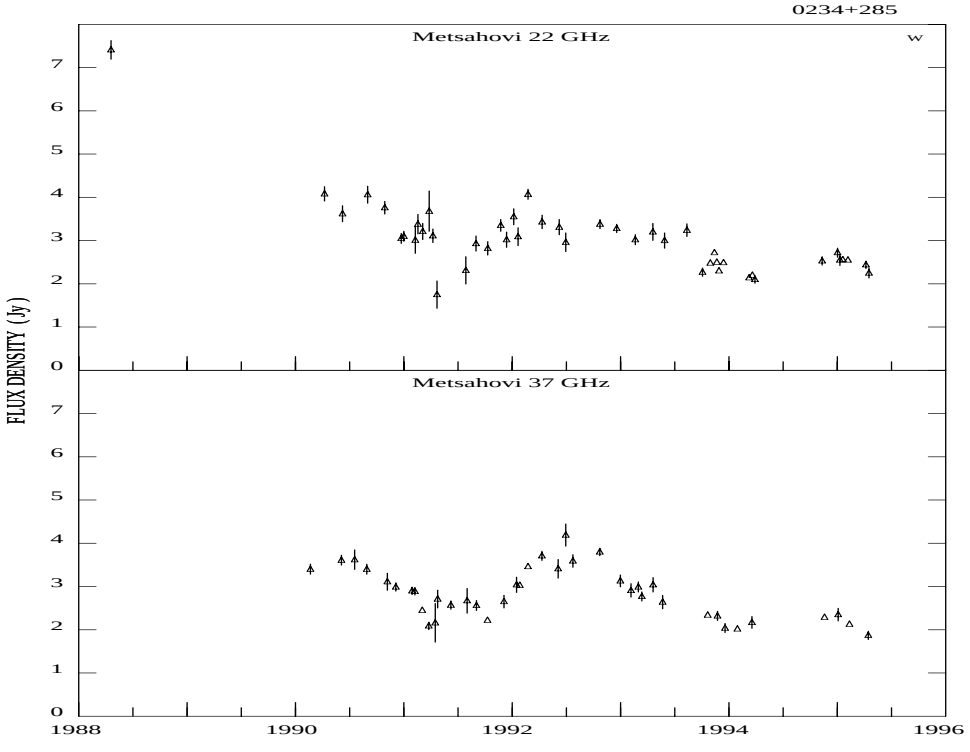

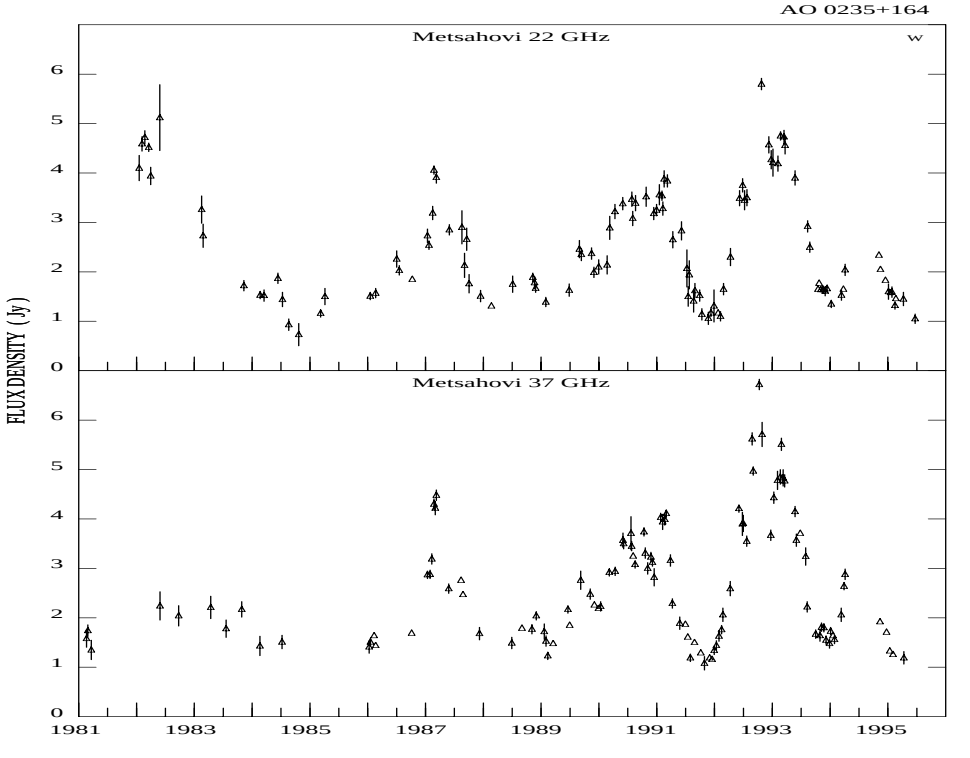

Fig. 1. continued

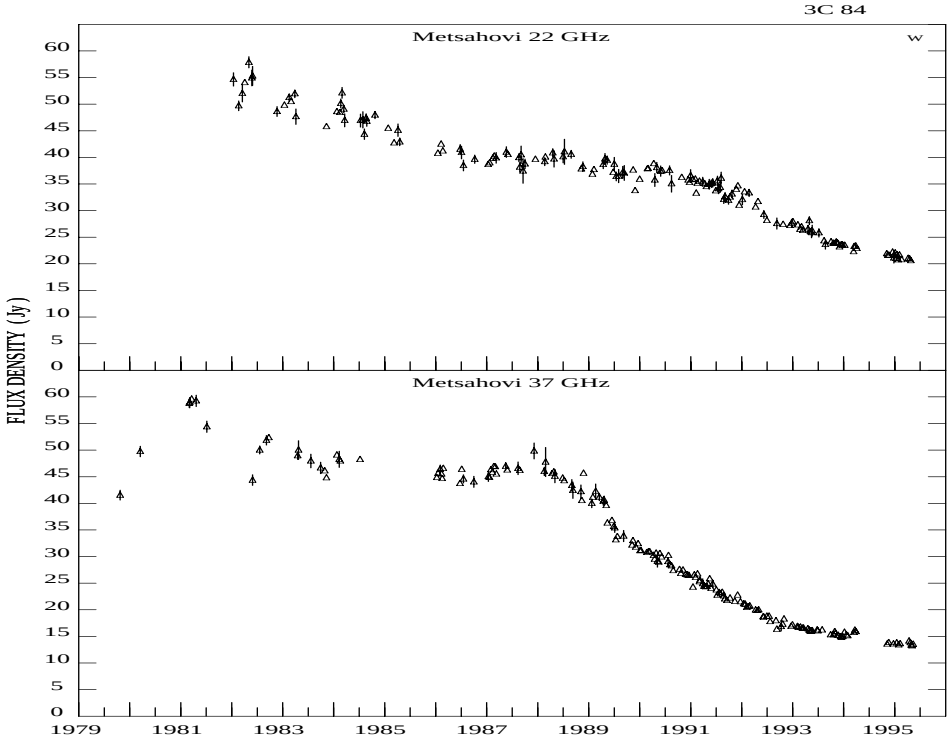

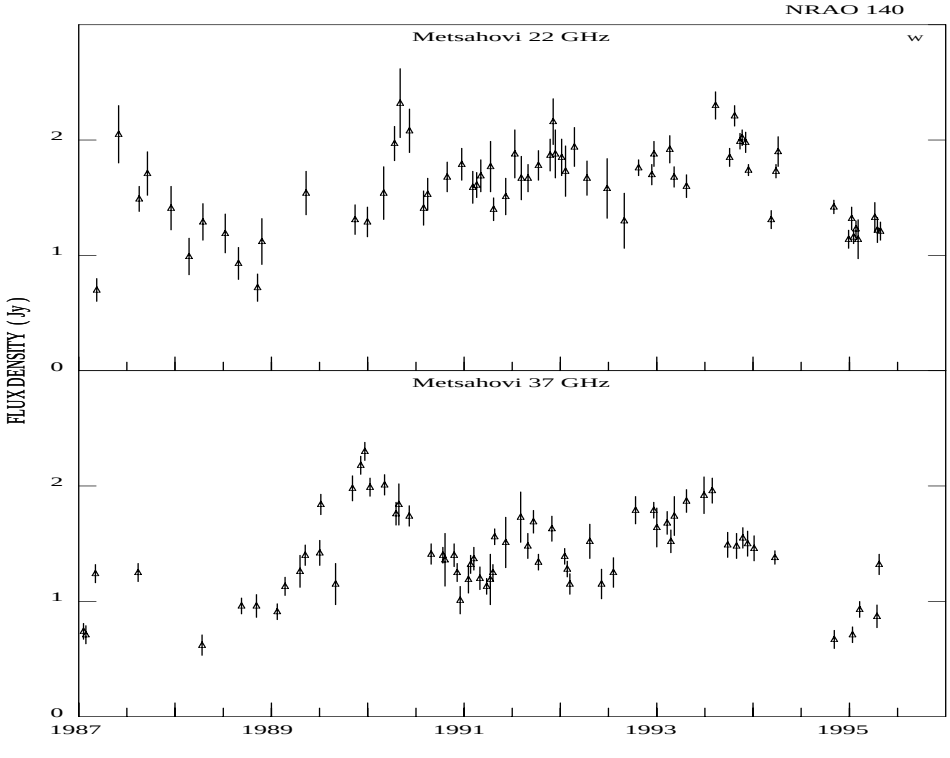

Fig. 1. continued

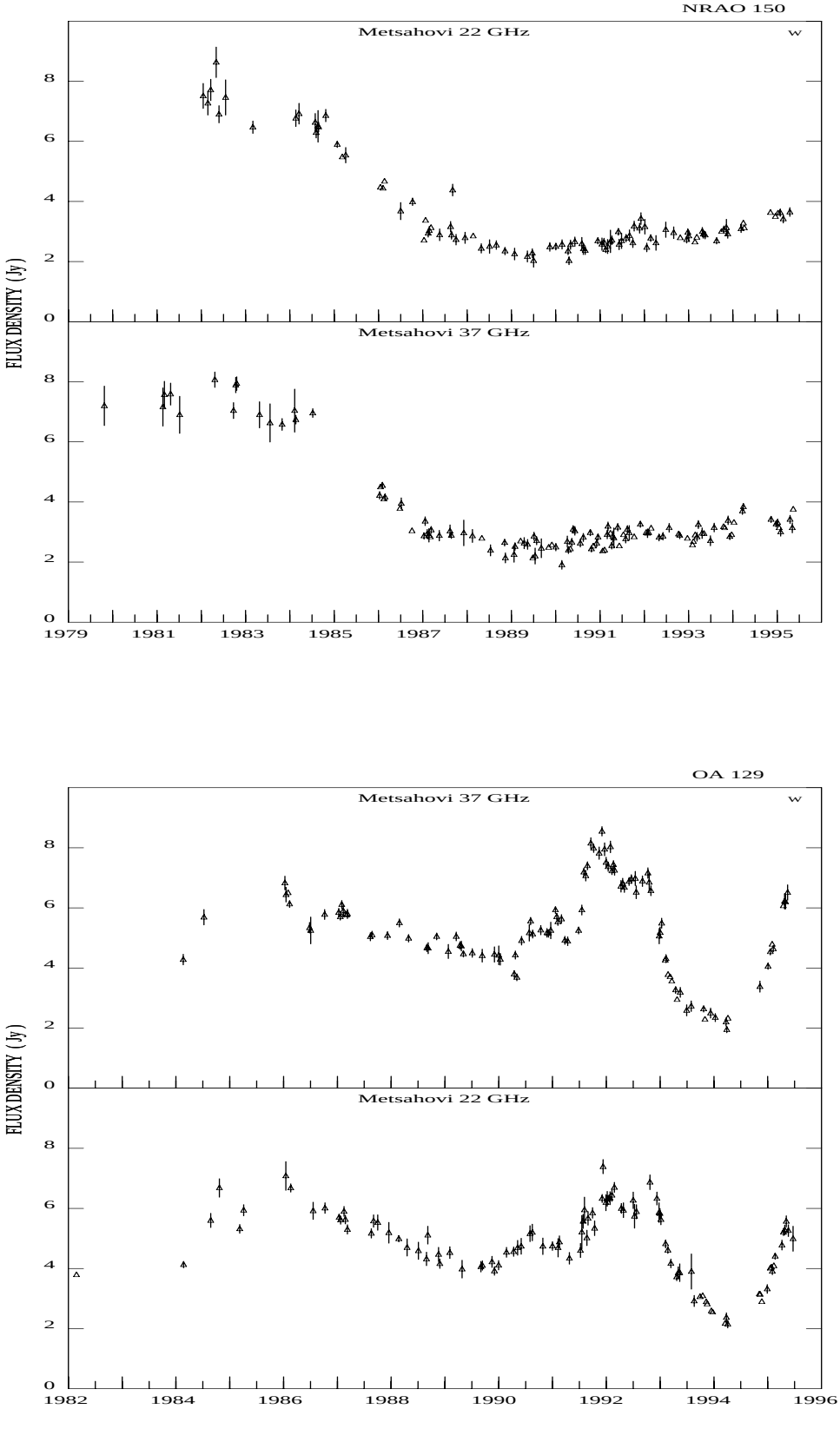

Fig. 1. continued

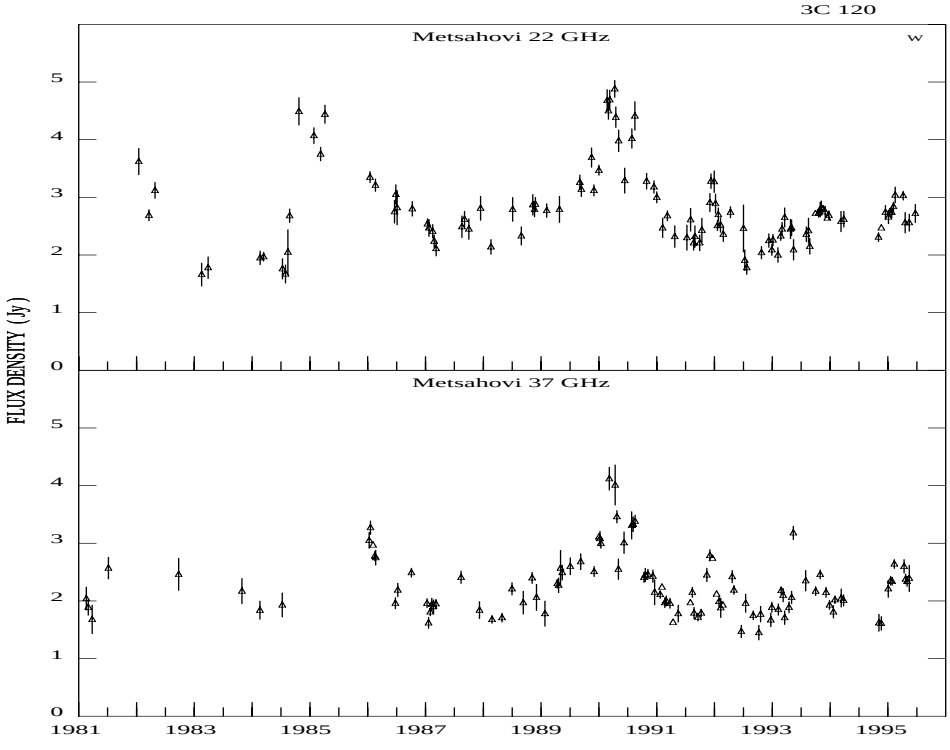

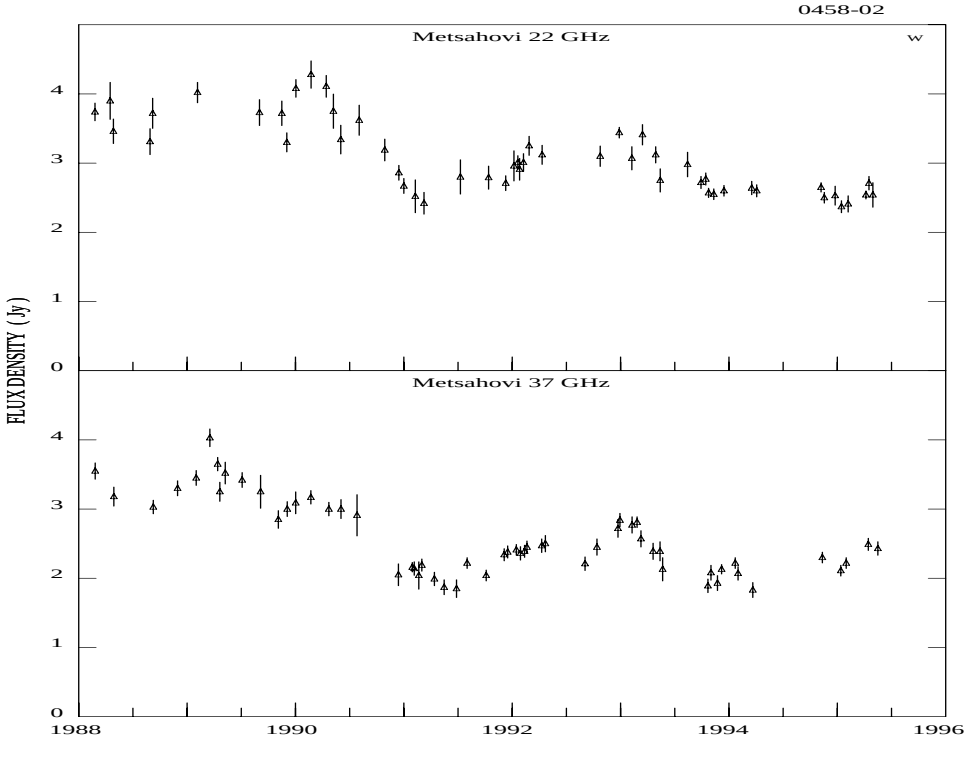

Fig. 1. continued

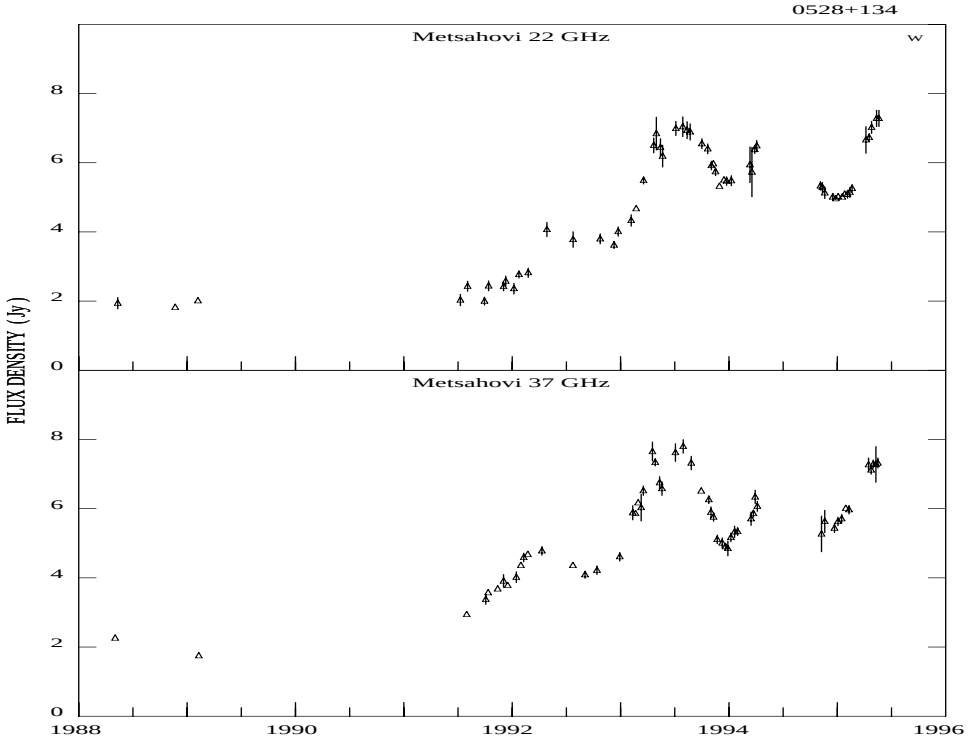

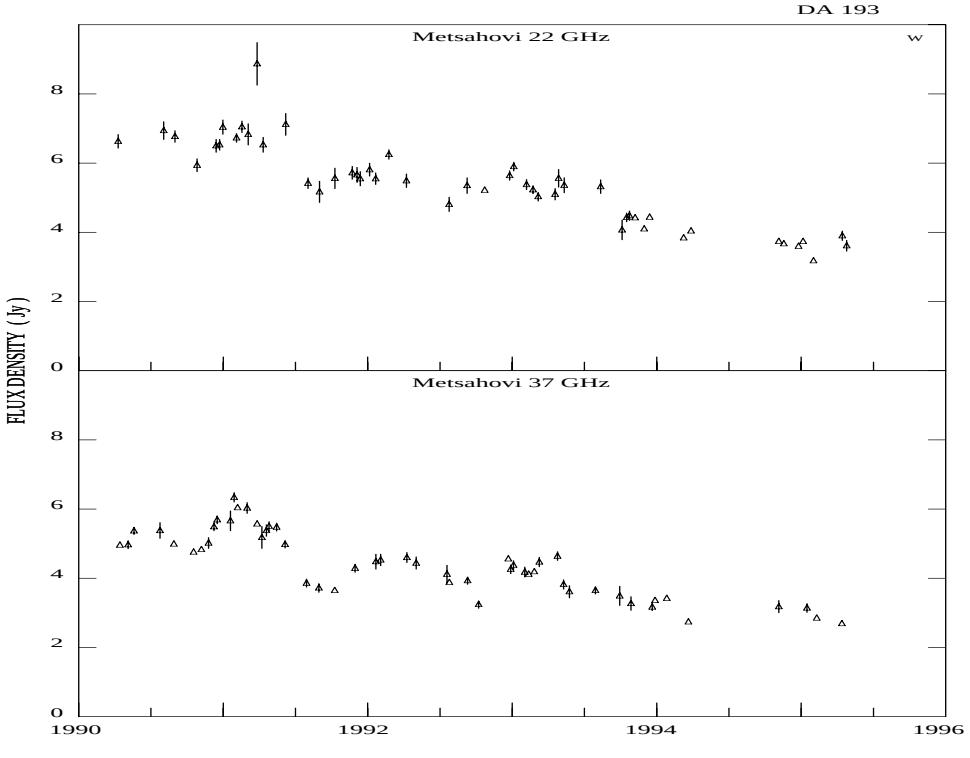

Fig. 1. continued

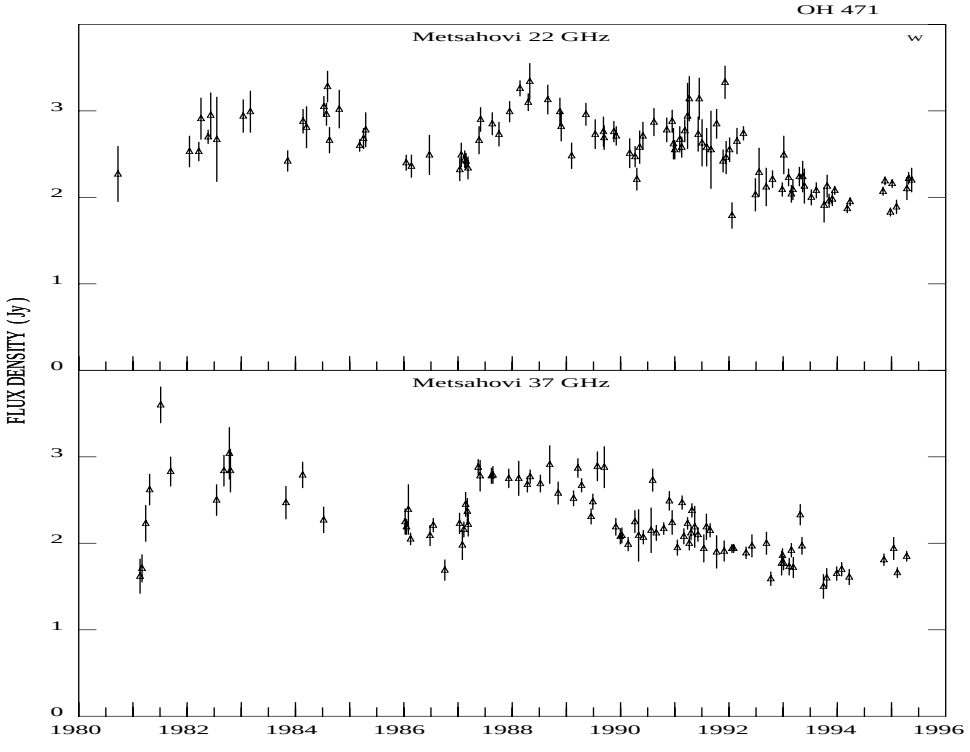

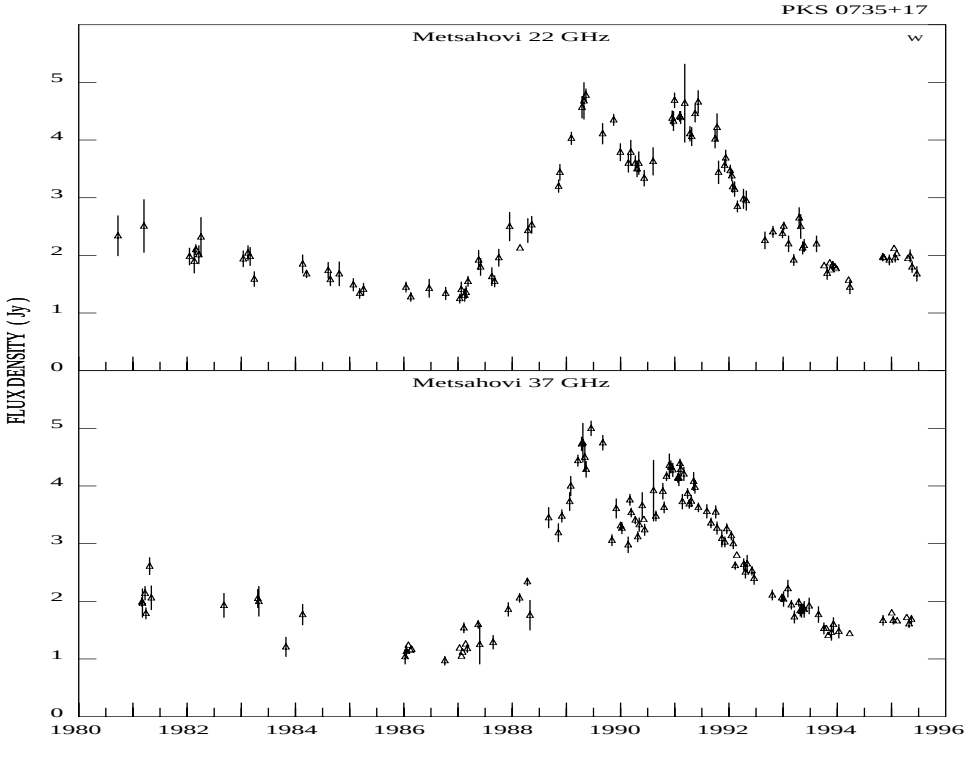

Fig. 1. continued

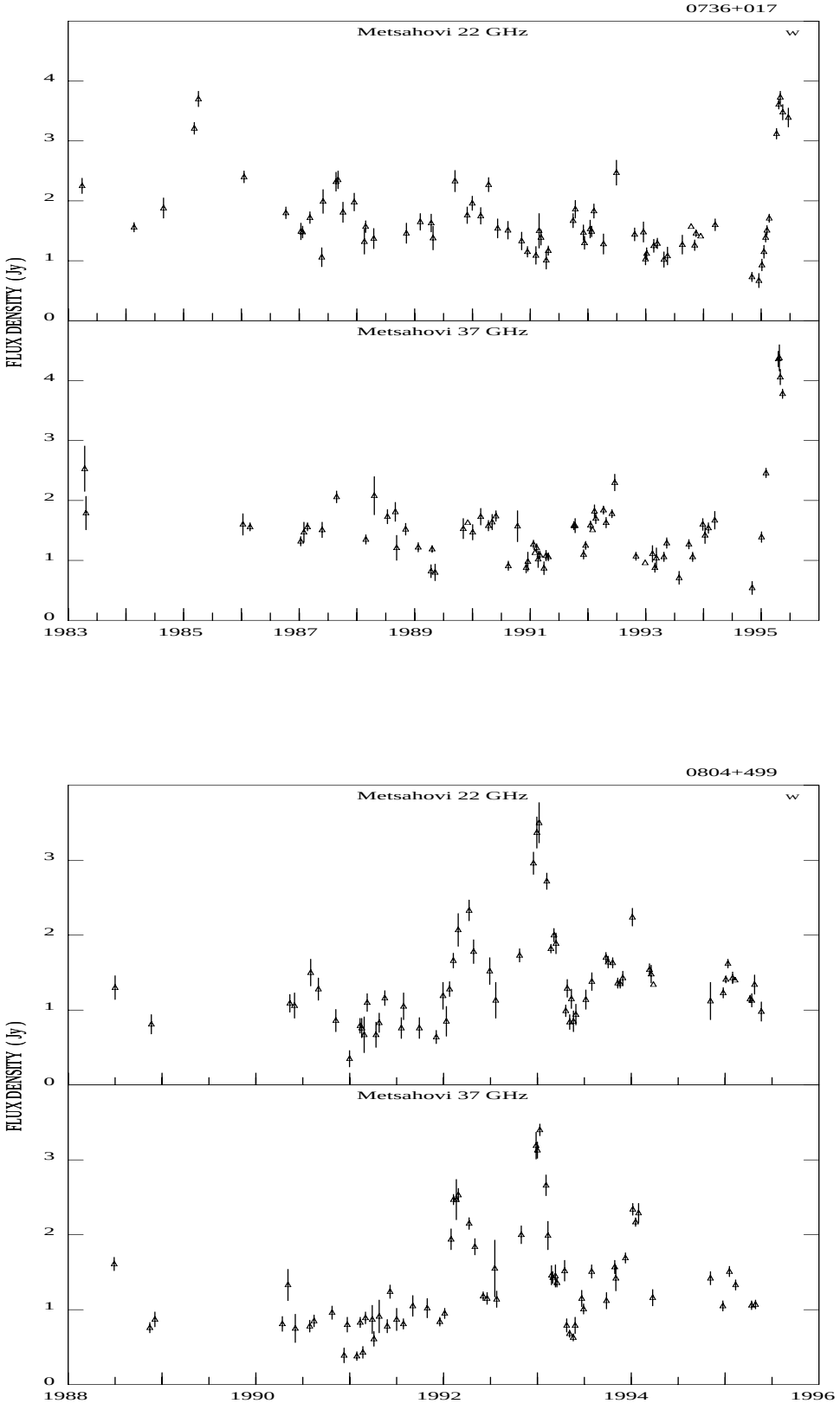

Fig. 1. continued

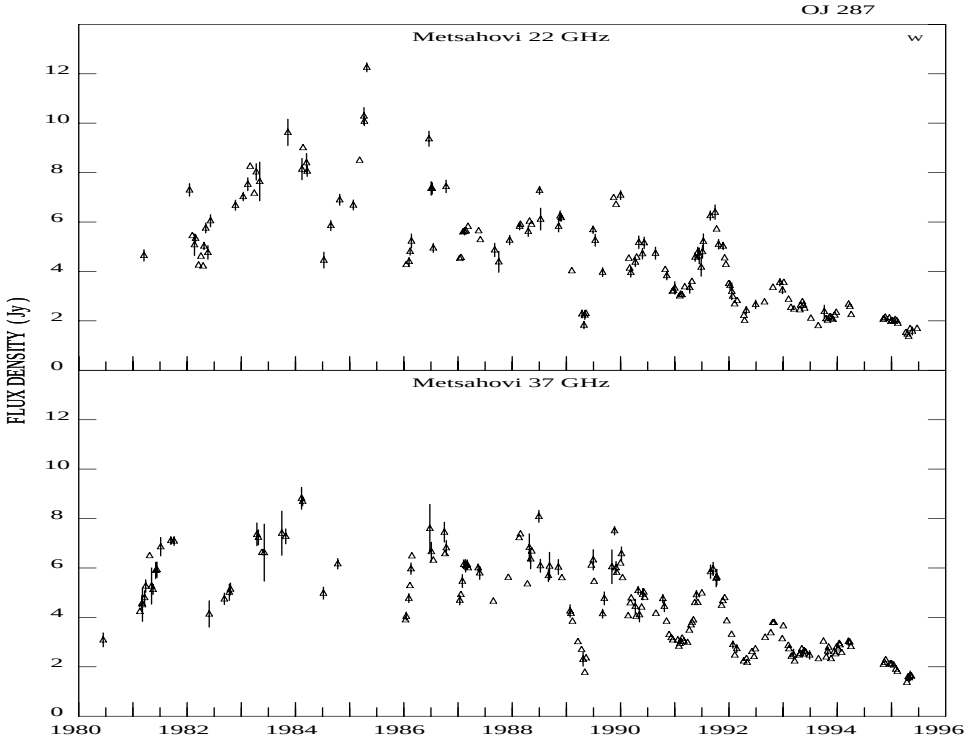

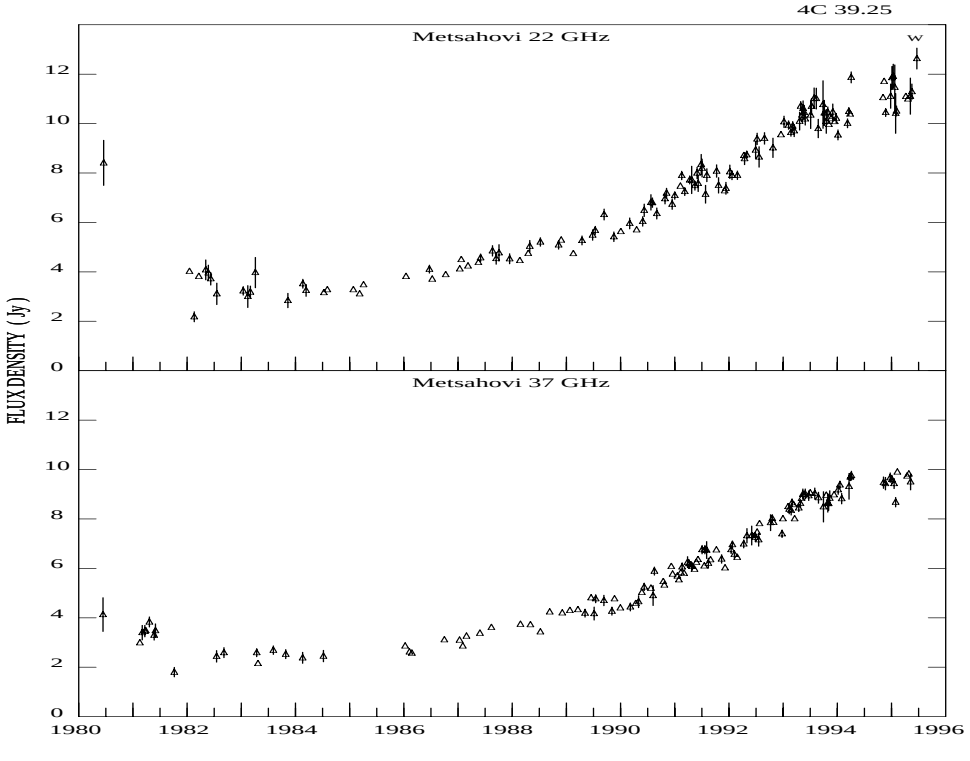

Fig. 1. continued

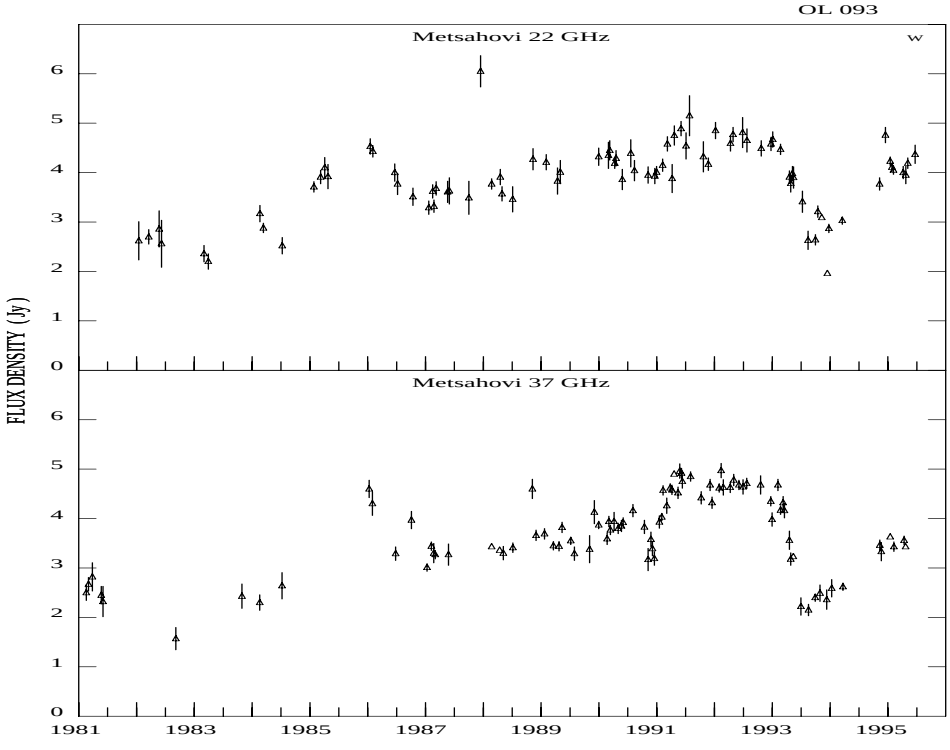

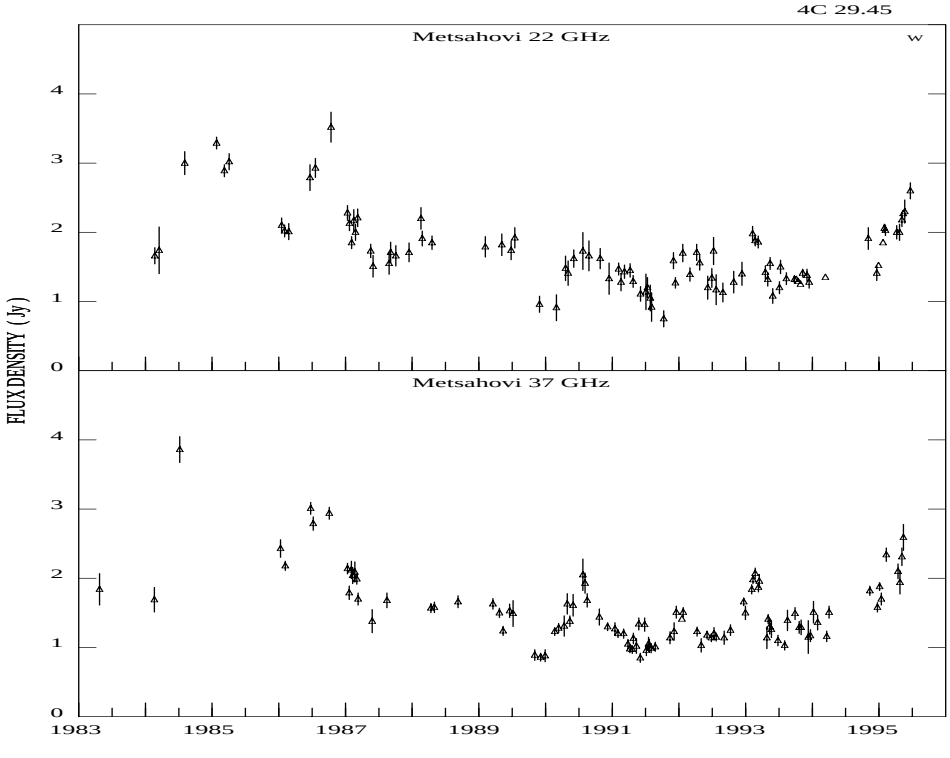

Fig. 1. continued

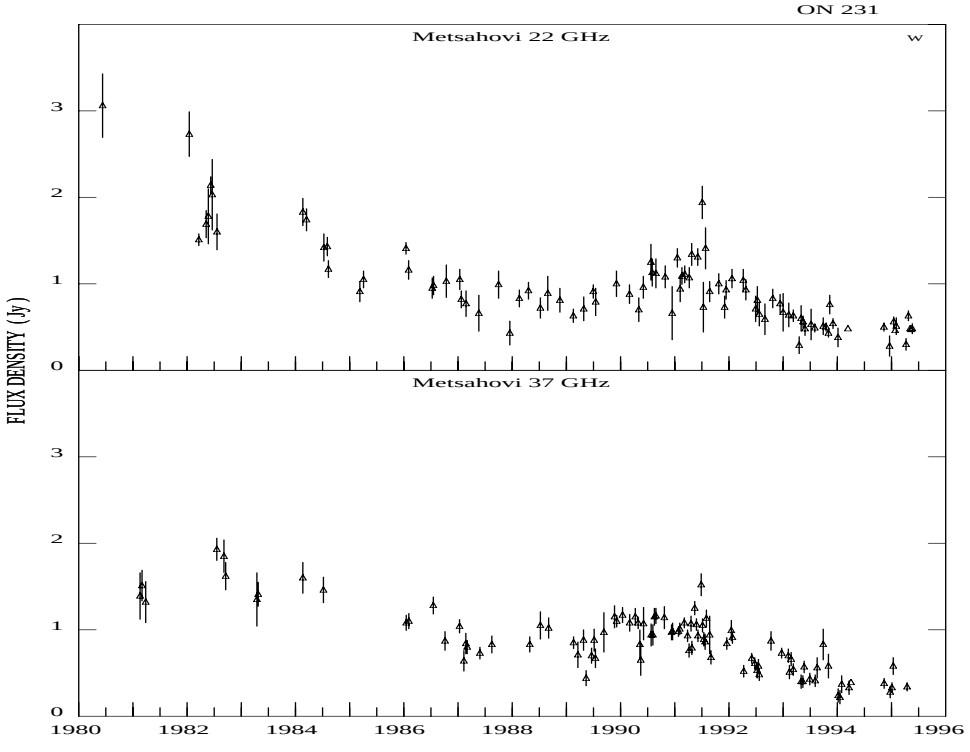

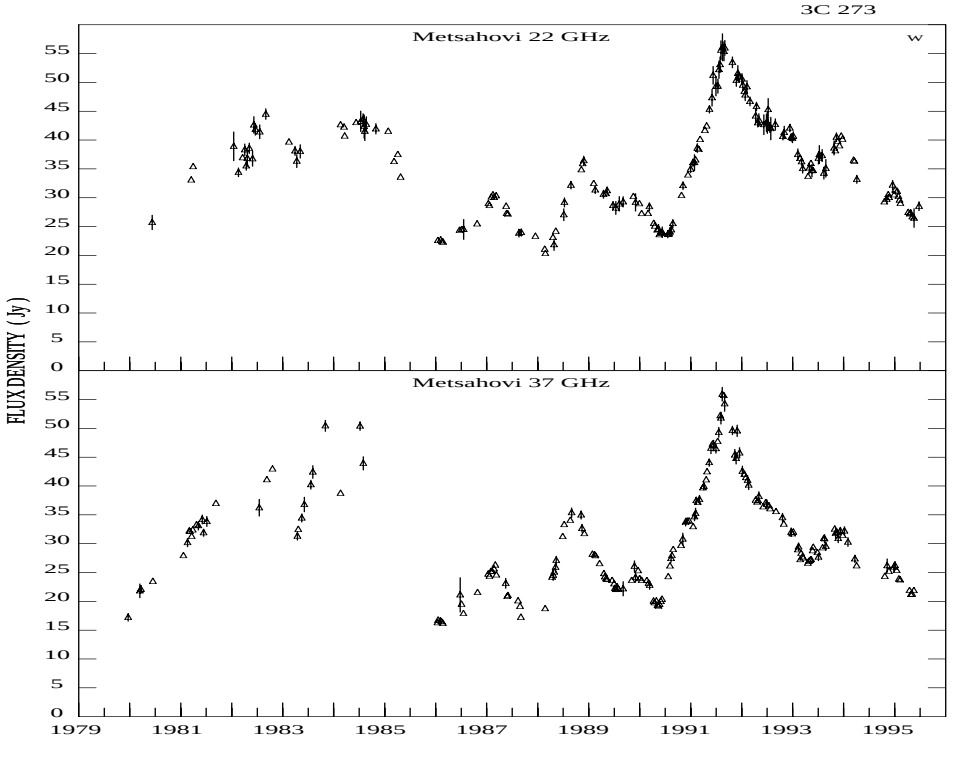

Fig. 1. continued

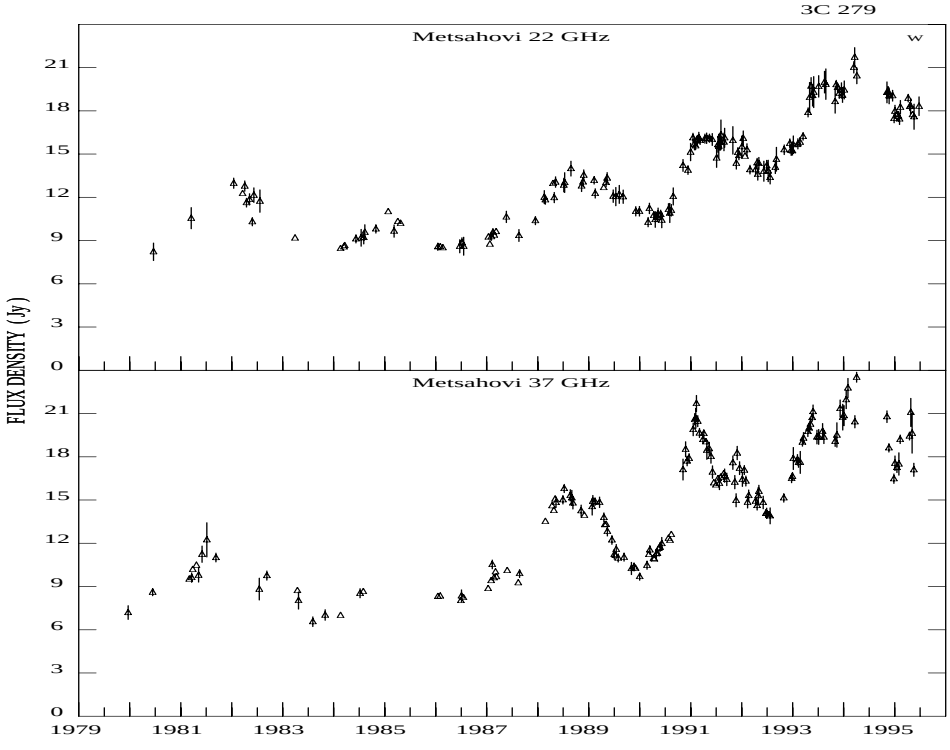

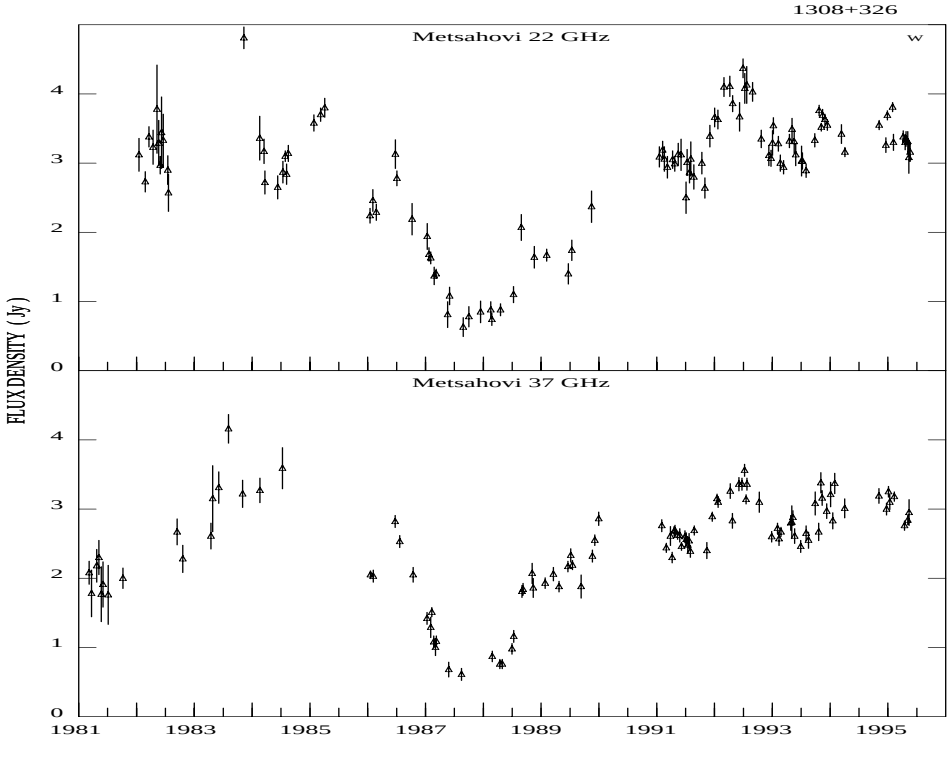

Fig. 1. continued

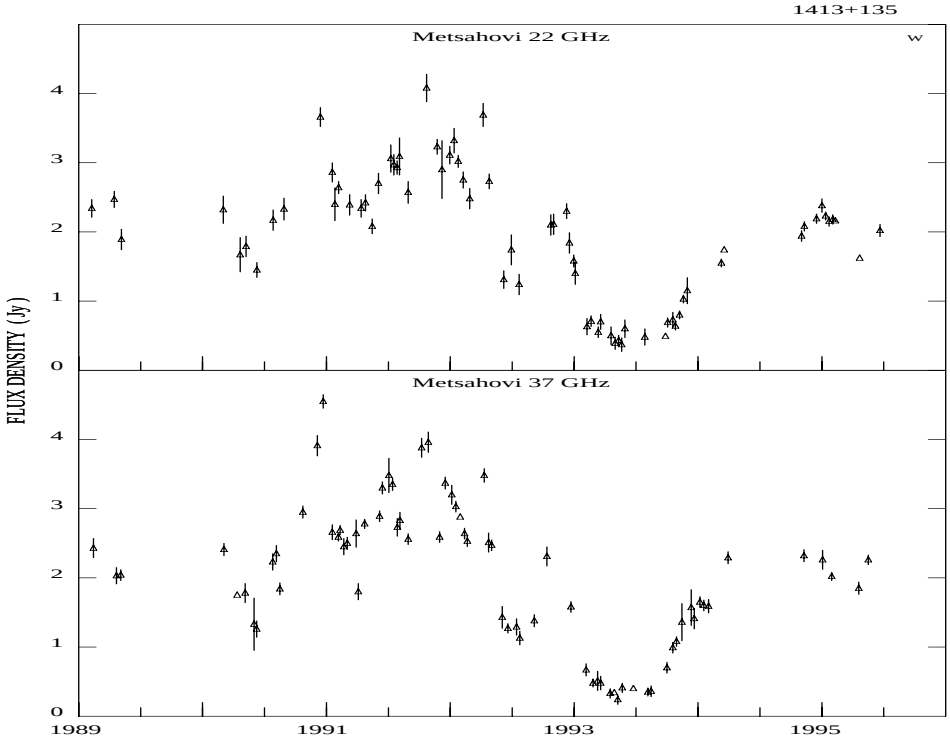

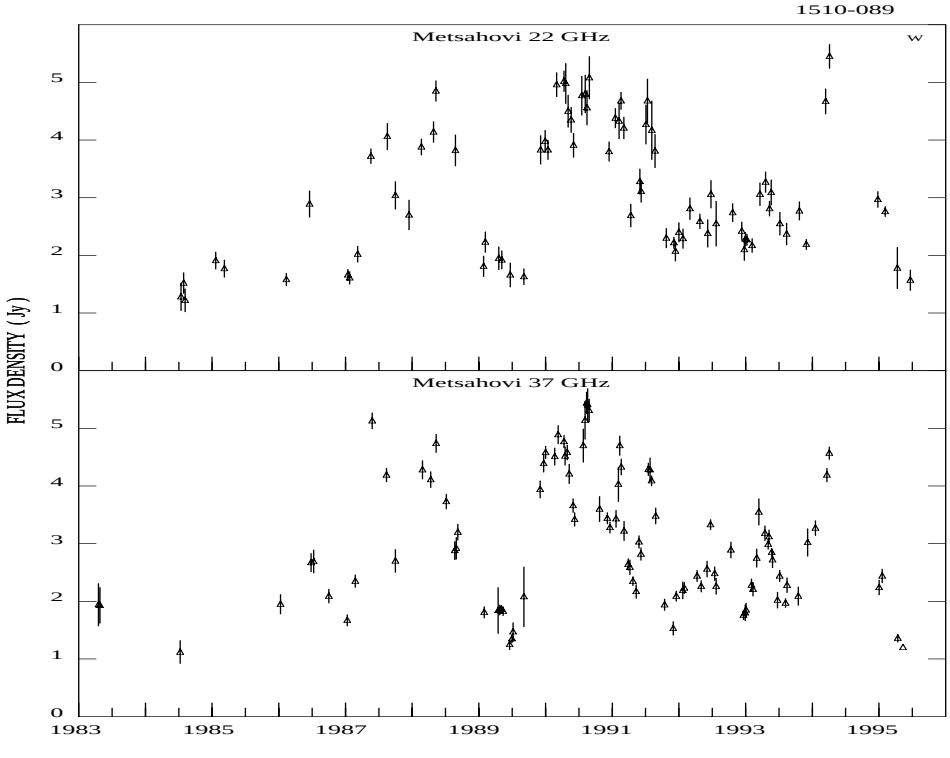

Fig. 1. continued

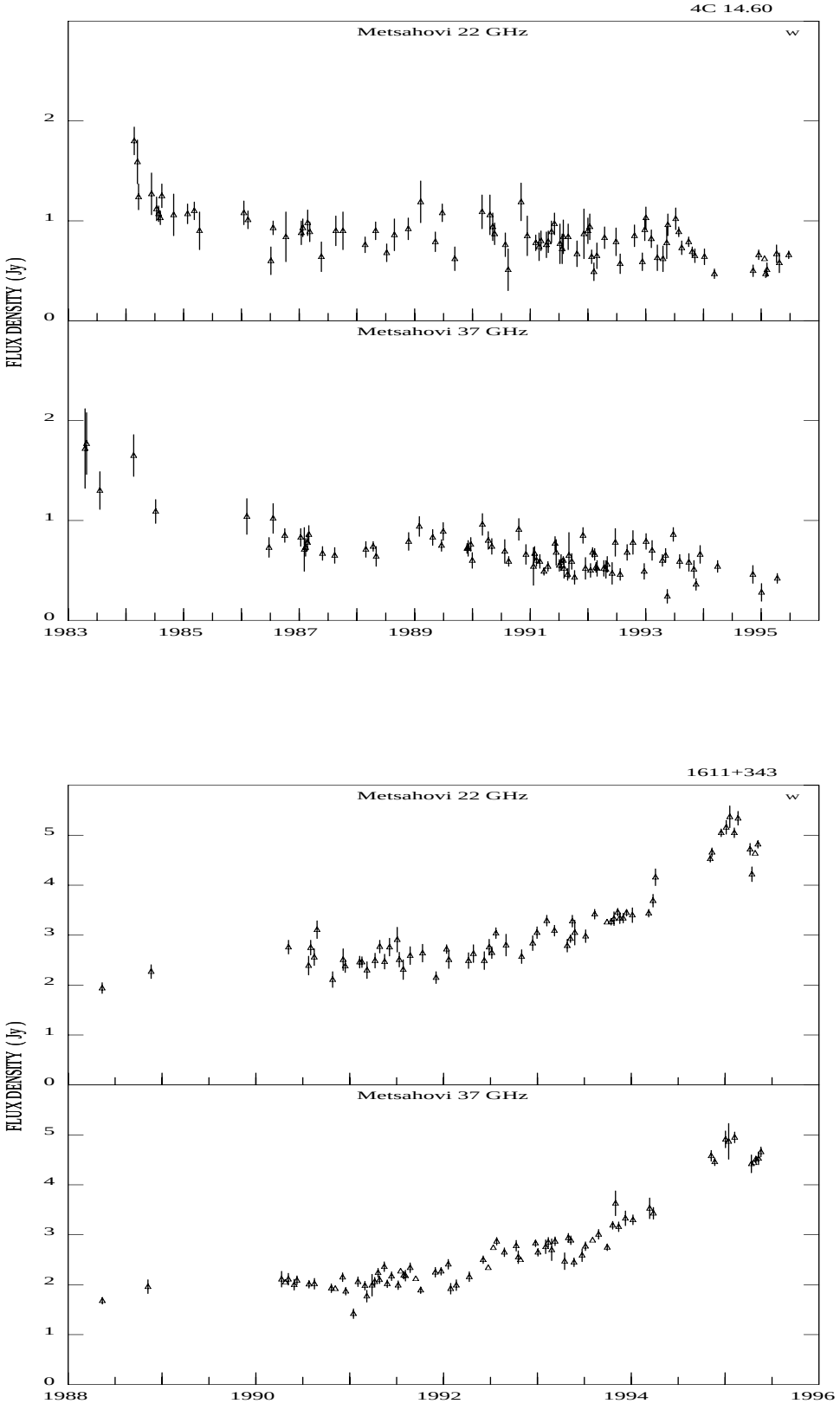

Fig. 1. continued

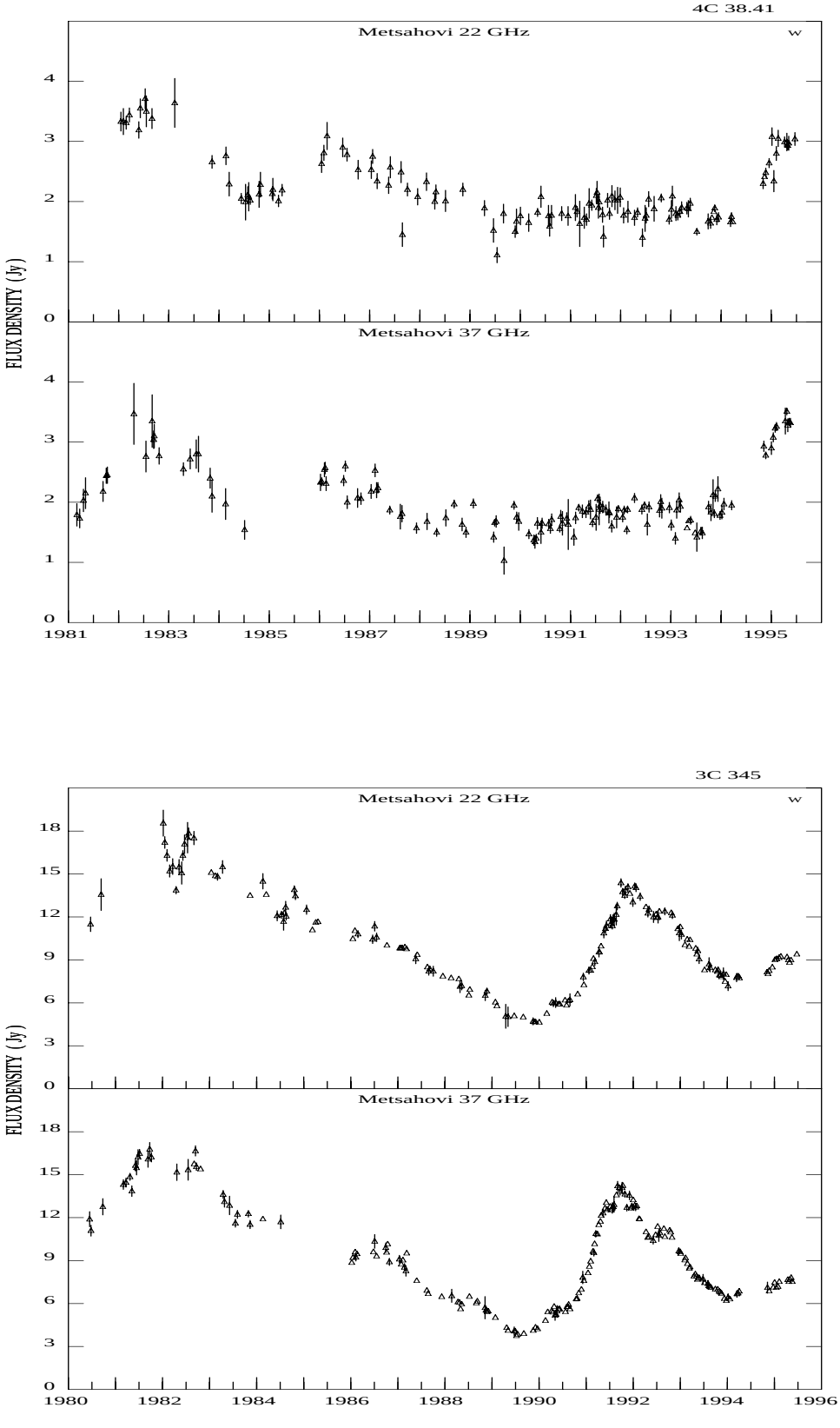

Fig. 1. continued

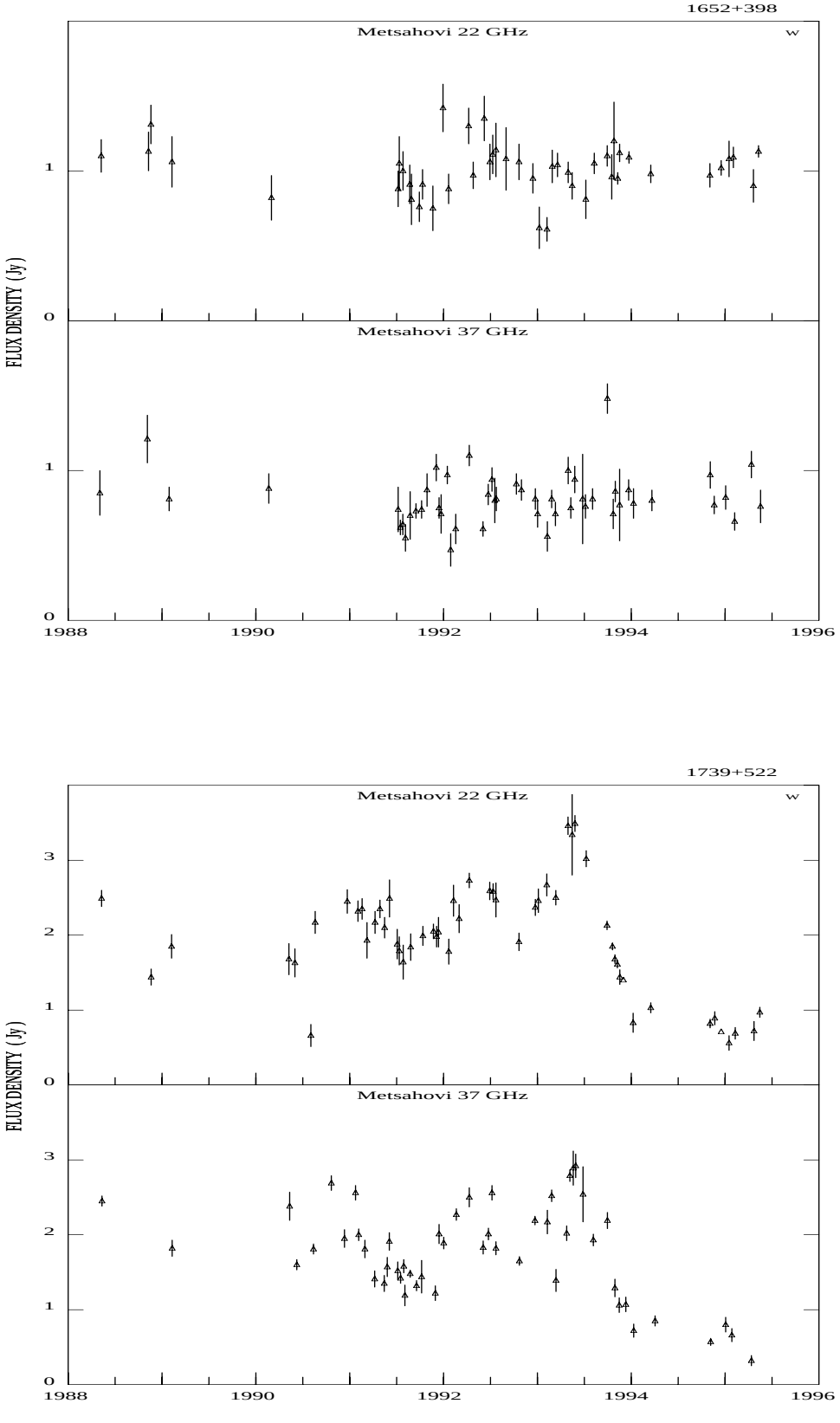

Fig. 1. continued

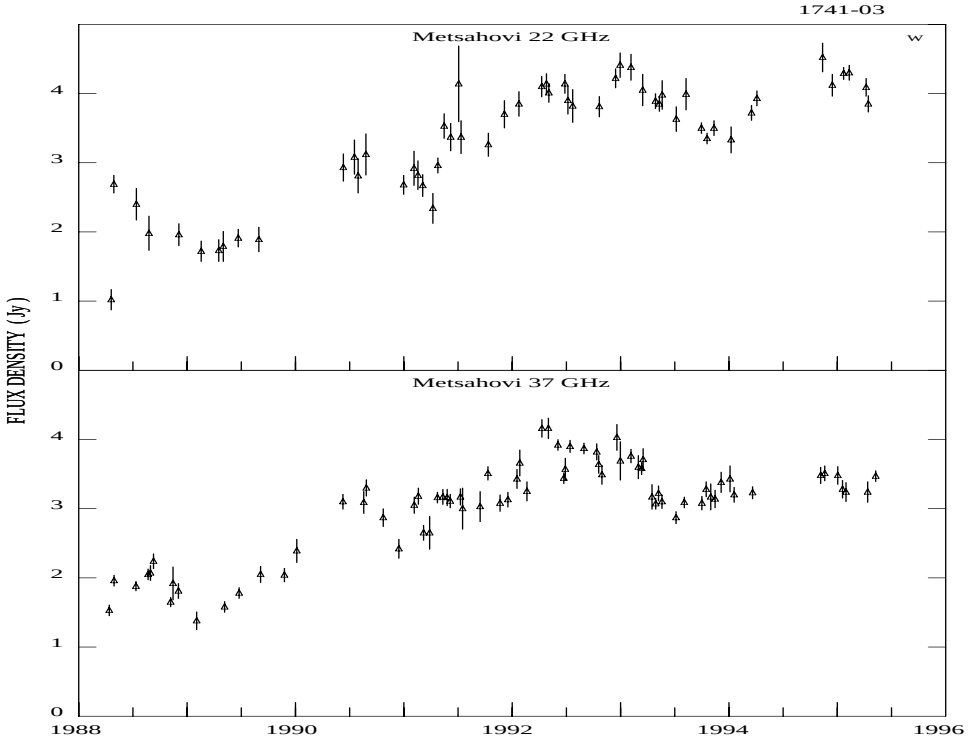

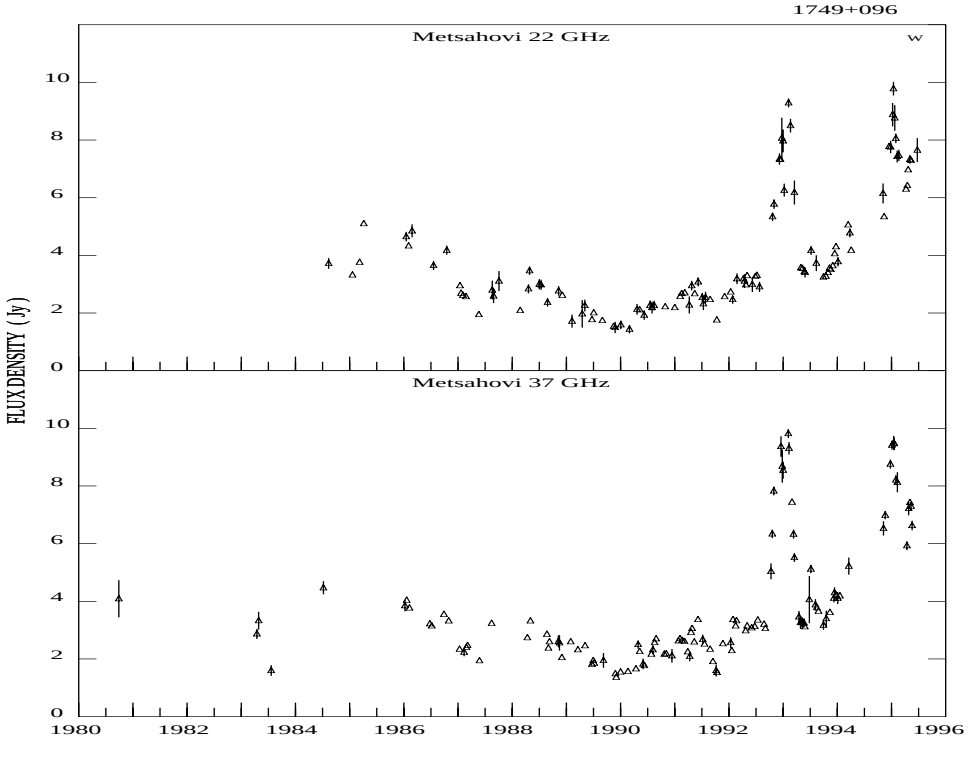

Fig. 1. continued

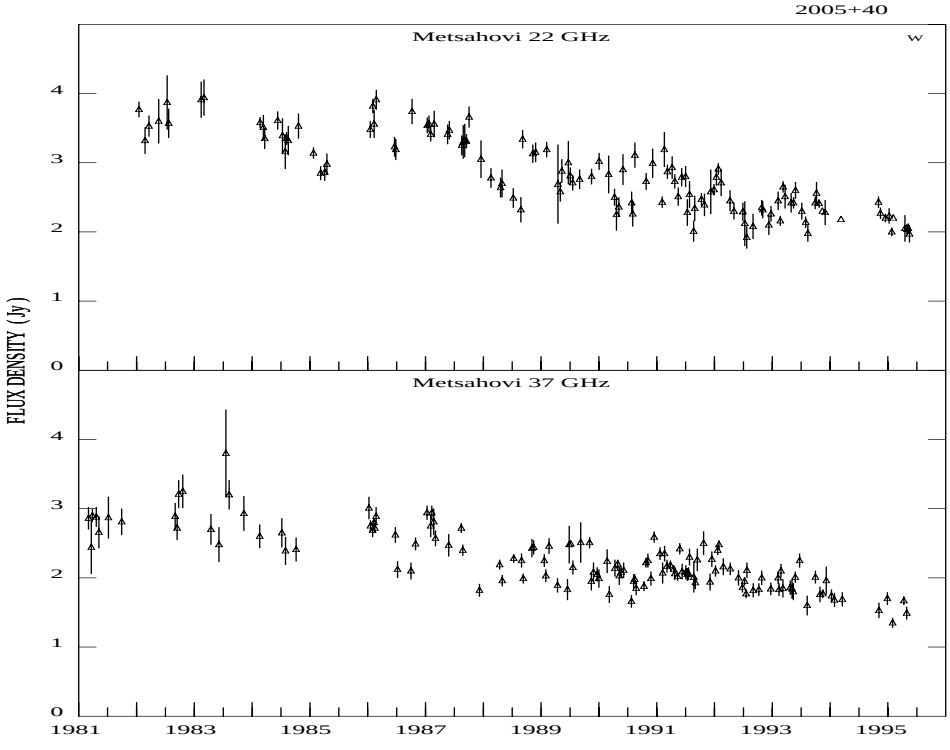

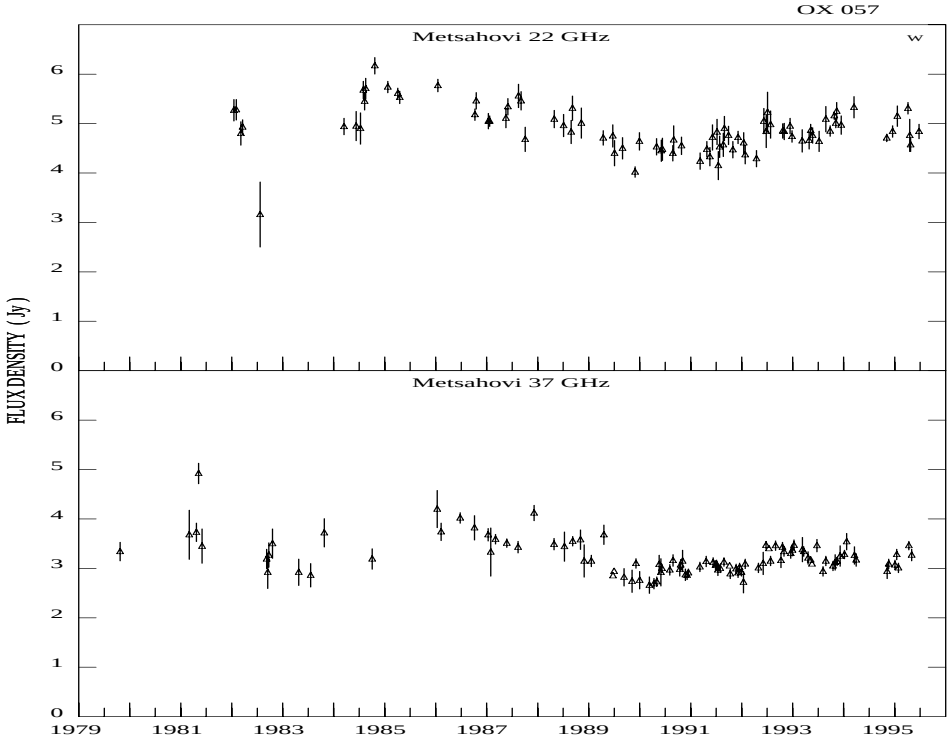

Fig. 1. continued

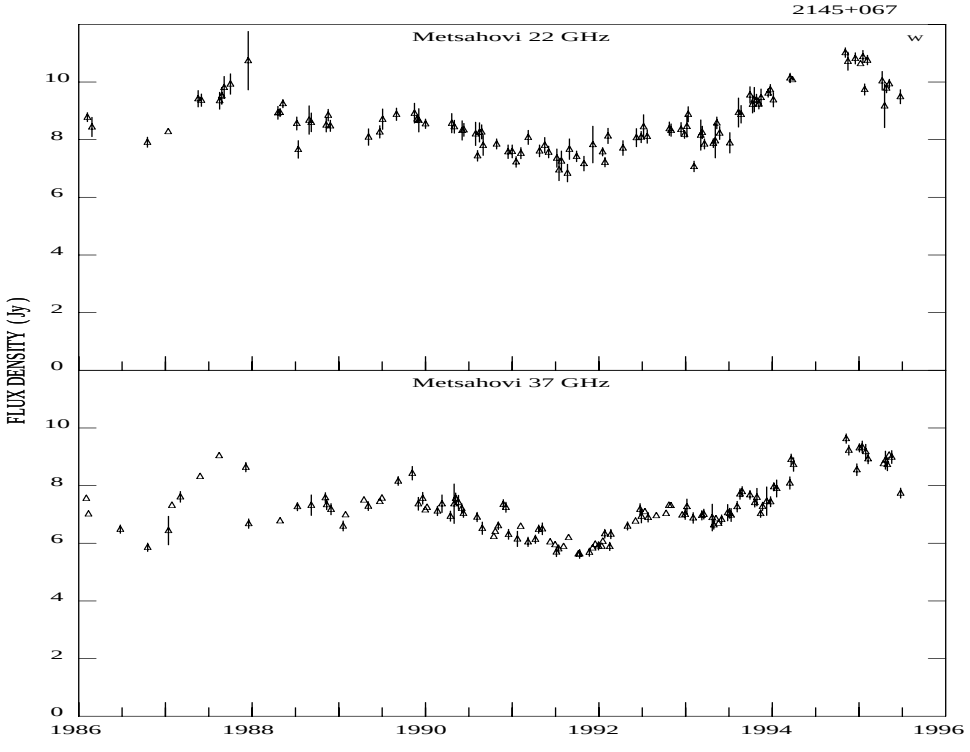

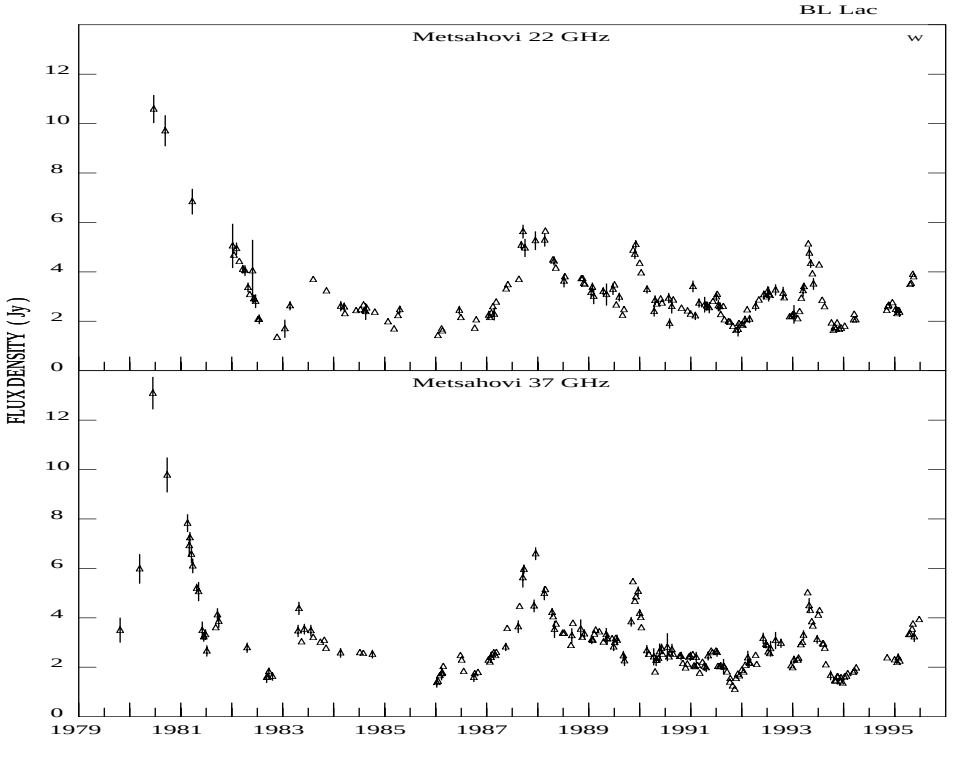

Fig. 1. continued

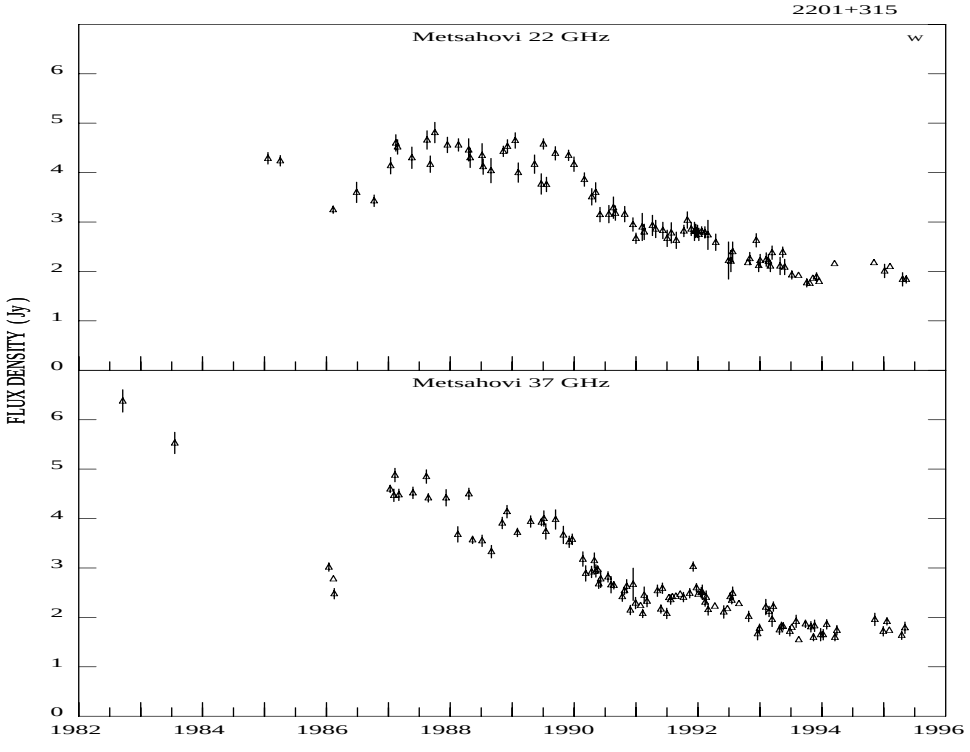

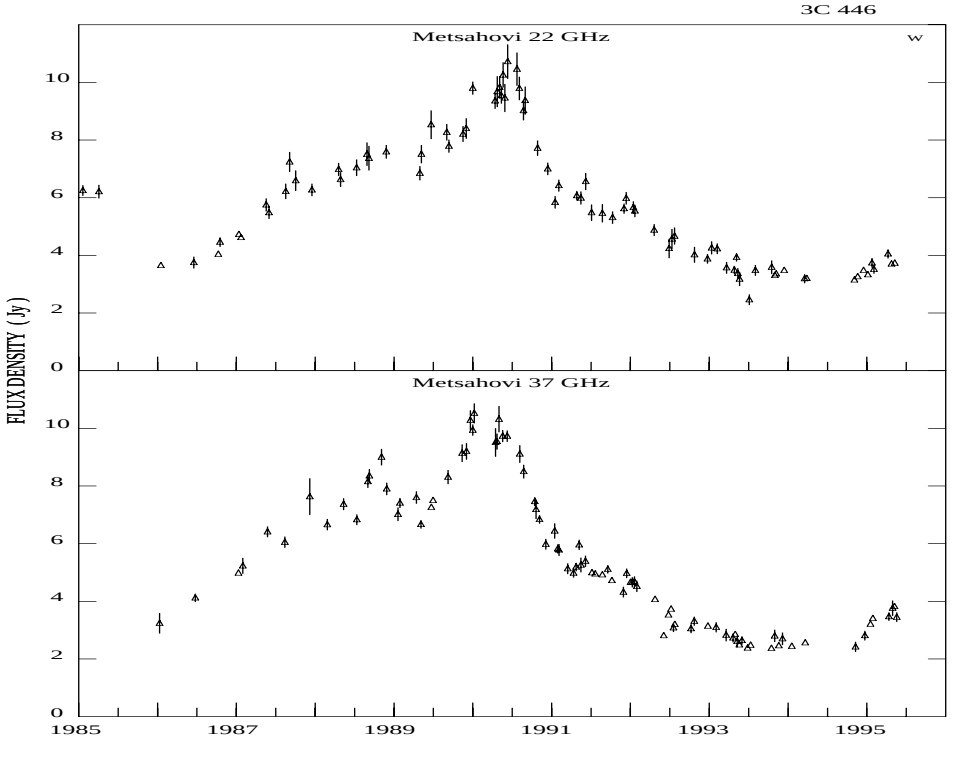

Fig. 1. continued

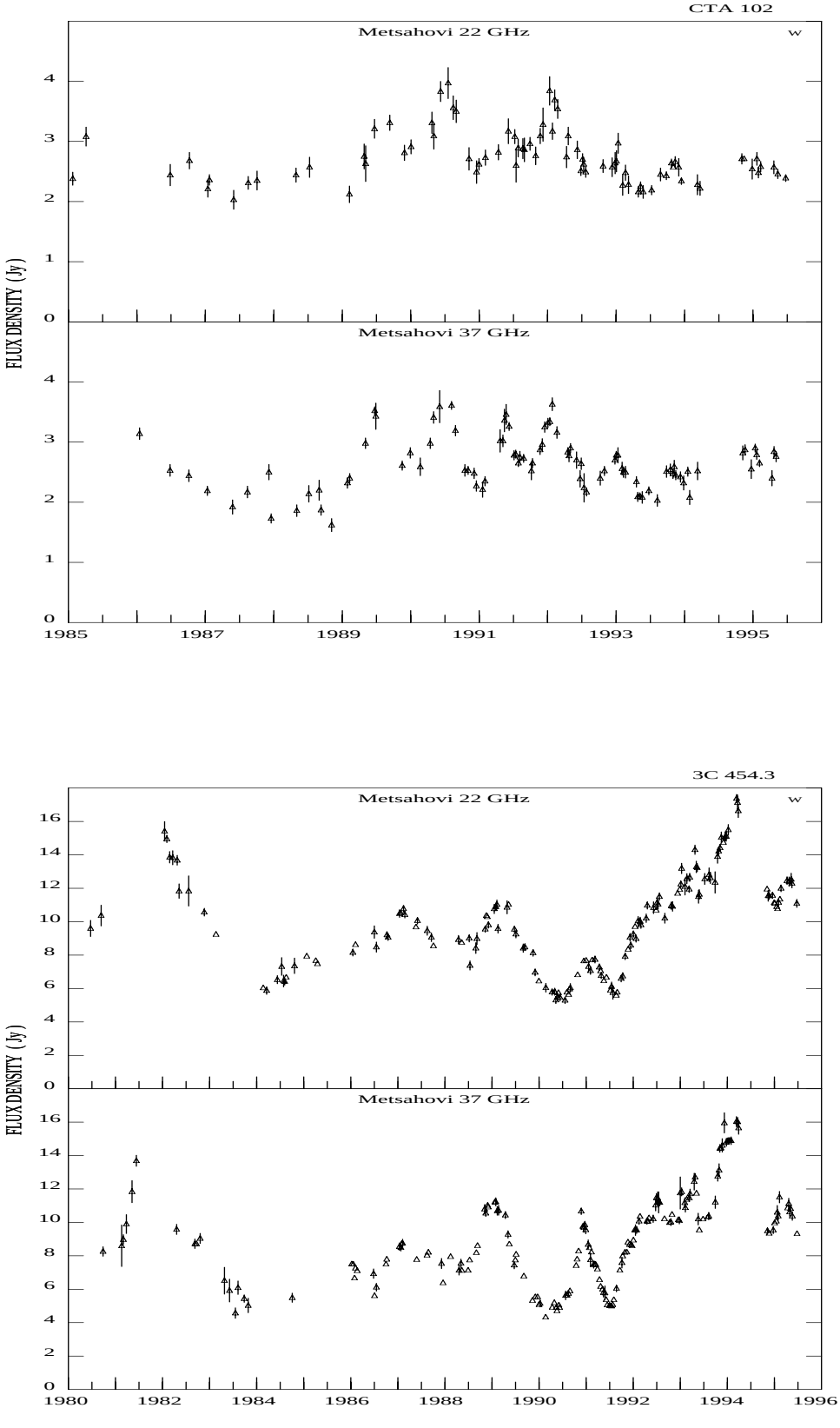

Fig. 1. continued